

DYNAMICS OF STOCHASTIC LOTKA-VOLTERRA PREDATOR-PREY MODELS DRIVEN BY THREE INDEPENDENT BROWNIAN MOTIONS

SHANGZHI LI, SHANGJIANG GUO

ABSTRACT. This article concerns the permanence and extinction of stochastic Lotka-Volterra predator-prey models perturbed by three independent white noises. We establish some criteria and present some numerical simulations that illustrate our theoretical results. It is shown that the presence of strong noise on either the intra-specific interaction rate or the inter-specific interaction rate may lead to complete different dynamical behaviors from the deterministic case.

1. INTRODUCTION

Predator-prey interaction is one of the basic interspecies relations in nature and society [3, 6, 11, 26]. Because of environmental stochastic perturbations, more and more researchers are interest on the following stochastic predator-prey model driven by three independent Brownian motions $W_1(\cdot)$, $W_2(\cdot)$ and $W_3(\cdot)$:

$$\begin{aligned}dX_1(t) &= X_1(t)(a_1 - b_1X_1(t) - c_1X_2(t))dt \\ &\quad + (\mu_1X_1^2(t) + \gamma_1X_1(t))dW_1(t) + \rho_1X_1(t)X_2(t)dW_3(t), \\dX_2(t) &= X_2(t)(a_2 - b_2X_2(t) + c_2X_1(t))dt \\ &\quad + (\mu_2X_2^2(t) + \gamma_2X_2(t))dW_2(t) + \rho_2X_1(t)X_2(t)dW_3(t).\end{aligned}\tag{1.1}$$

where $X_1(t)$ and $X_2(t)$ denote the quantities of prey and predator populations, respectively, a_1 and a_2 are intrinsic growth rates, positive constants b_1 and b_2 represent the intra-specific interaction rates, positive constants c_1 and c_2 represent the inter-specific interaction. More precisely, c_1 is the death rate per encounter of prey due to predation, and c_2/c_1 is the efficiency of turning predated prey into predator. The dynamics of (1.1) without noise (i.e., $\mu_j = \gamma_j = \rho_j = 0$ for $j = 1, 2$) is quite simple [1, 22]. However, the presence of noise makes (1.1) have more complicated dynamical behaviour. For example, in [2, 9, 30, 32]) there are a plenty of results on the stochastic predator-prey model

$$\begin{aligned}dX_1(t) &= X_1(t)(a_1 - b_1X_1(t) - c_1X_2(t))dt + \gamma_1X_1(t)dW(t), \\dX_2(t) &= X_2(t)(-a_2 - b_2X_2(t) + c_2X_1(t))dt + \gamma_2X_2(t)dW(t),\end{aligned}\tag{1.2}$$

2020 *Mathematics Subject Classification*. 34C12, 60H10, 92D25.

Key words and phrases. Predator-prey model; Lyapunov exponent; permanence; extinction.

©2022. This work is licensed under a CC BY 4.0 license.

Submitted March 21, 2021. Published April 20, 2022.

where all the parameters are positive and the intrinsic growth rates are perturbed stochastically. Arnold, Horsthemke and Stucki [2] investigated the sample paths of equation (1.2). Rudniki et al [27, 28, 29] investigated the convergence of densities of the distributions of the solutions of (1.2). Mao, Sabanis and Renshaw [21] investigated the existence and uniqueness of the positive solution of the following model, where the intra-specific interaction rates are perturbed stochastically,

$$\begin{aligned} dX_1(t) &= X_1(t)(a_1 - b_1X_1(t) - c_1X_2(t))dt + \mu_1X_1^2(t)dW(t), \\ dX_2(t) &= X_2(t)(-a_2 - b_2X_2(t) + c_2X_1(t))dt + \mu_2X_2^2(t)dW(t). \end{aligned} \quad (1.3)$$

Dang, Du, and Ton [5] proved that the densities of (1.3) either converge in L^1 to an invariant density or converge weakly to a singular measure on the boundary as well. It is natural to ask what happens to dynamical behaviour of model (1.1) in which there are noises and perturbations on both inter-specific interaction rates intra-specific interaction rates. As we know, there are few literatures in this direction. For convenience, by assuming $\gamma_1 = \gamma_2 = 0$ we shall investigate the system

$$\begin{aligned} dX_1(t) &= X_1(t)(a_1 - b_1X_1(t) - c_1X_2(t))dt \\ &\quad + \mu_1X_1^2(t)dW_1(t) + \rho_1X_1(t)X_2(t)dW_3(t), \\ dX_2(t) &= X_2(t)(a_2 - b_2X_2(t) + c_2X_1(t))dt \\ &\quad + \mu_2X_2^2(t)dW_2(t) + \rho_2X_1(t)X_2(t)dW_3(t). \end{aligned} \quad (1.4)$$

Stochastic perturbations on intrinsic growth rates a_1 and a_2 will be investigated in our another paper.

Much effort has been devoted to the study of prey-predator systems with $a_1 > 0 > a_2$ (that is, the intrinsic growth rate of the prey population is positive while the intrinsic growth rate of the predator population is negative); See, for example, [5, 10, 16, 21]. In such prey-predator systems, the predator population relies on a single species for food. In a real world, most species feed on more than one species. Therefore, in this paper we shall not confine our attention only to the case where $a_1 > 0 > a_2$ and shall distinguish four cases (i.e., $a_1 < 0$ and $a_2 < 0$, $a_1 < 0 < a_2$, $a_1 > 0 > a_2$, $a_1 > 0$ and $a_2 > 0$) to investigate the dynamics of system (1.4). To make the ecological model more accurate, we consider three different white noises in one model, since both the intra-specific interaction rates and inter-specific interaction rates might be perturbed by environmental randomness.

One of important concepts in stochastic population models is stochastic permanence, which indicates that the species will survive forever. Thus, another purpose is to describe the effect of the three white noises on the stochastic permanence of (1.4). In particular, we want to see whether and how large intensities of noises could lead to extinction even though the population persists in the associated deterministic system, and also to see whether and how large intensities of noises could lead to the permanence of the population even though some population dies out in the associated deterministic system.

Finding conditions ensuring the stochastic permanence is drawing plenty of attentions (see, for example, [10]). Some useful methods such as Lyapunov-type functions and ergodicity have been proposed [8, 17]. Thus, it is interesting to develop much sharper or more general criteria by formulating more general and better candidates for Lyapunov functions. Recently, Nguyen and Yin [23] studied the coexistence and exclusion of stochastic competitive Lotka-Volterra models by establishing a threshold in terms of dynamics on the boundary. Different from

the Lyapunov method, in this paper we shall develop Nguyen and Yin's approach in [23] and introduce two thresholds λ_1 and λ_2 to determine the permanence and extinction in stochastic prey-predator system (1.4). In particular, we know that Lotka-Volterra models laid a theoretical foundation for competition among species [13, 18, 19]. Here, we should point out that our approach is applicable for a variety of other stochastic Lotka-Volterra competition models.

Let $(\Omega, \mathcal{F}, \{\mathcal{F}\}_{t \geq 0}, \mathbb{P})$ be a complete filtered probability space with the filtration $\{\mathcal{F}\}_{t \geq 0}$. We suppose that $\mu_i \neq 0$, $i = 1, 2$, so that the diffusion is non-degenerate. Let $\bar{X}_x(t) = (X_{1,x}(t), X_{2,x}(t))$ be the solution to (1.4) with initial value $x = (x_1, x_2)$. Denote that $\mathbb{R}_+^{2,\circ} = \{(x_1, x_2) : x_1 > 0, x_2 > 0\}$. Throughout this paper, suppose that $\mu_i > 0$, $\rho_i \geq 0$, $i = 1, 2$. For each $x \in \mathbb{R}_+^{2,\circ}$, it is proved in [20] that the solution $X_x(t)$ remains in $\mathbb{R}_+^{2,\circ}$ with probability 1. It is easy to see that the solution $X_x(t)$ is a Markov process.

This article is organized as follows. In Section 2, we investigate the dynamics on the boundary of the solutions and then derive some thresholds that are used to determine extinction and permanence. In particular, we state our main theoretical results and describe the main difference between the stochastic system (1.4) and its associated deterministic system. In Section 3, we perform some numerical simulations to illustrate our theoretical results. Section 4 is devoted to the proof of the extinction and weak convergence to a boundary distribution of species of system (1.4) with $a_1 < 0$. Section 5 is devoted to the dynamics of system (1.4) with $a_1 > 0 > a_2$. In Section 5, we provide the proof of the weak convergence to a boundary distribution and coexistence of the species of (1.4) in the case where $a_1 > 0$ and $a_2 > 0$.

2. MAIN RESULTS

To state our main result, we need to introduce an auxiliary process. For each fixed $j = 1, 2$, consider

$$d\psi(t) = \psi(t)(a_j - b_j\psi(t))dt + \mu_j\psi^2(t)dW_j(t), \quad (2.1)$$

where $W_1(t)$ and $W_2(t)$ are defined as in (1.4). Let $\psi_{j,x}$ be the solution to (2.1) starting at x_j . Equation (2.1) with $a_j > 0$ has a unique invariant probability measure π_j^* in $(0, \infty)$ with density (see [5] for more details)

$$f_j^*(\phi) = \frac{c_j^*}{\phi^4} \exp\left(\frac{2b_j}{\mu_j^2\phi} - \frac{a_j}{\mu_j^2\phi^2}\right) \quad \text{for } \phi > 0.$$

Here c_j^* is a normalizing constant. Moreover, for every $x > 0$ and $p < 3$,

$$\mathbb{P}\left\{\lim_{T \rightarrow \infty} \frac{1}{T} \int_0^T \psi_{j,x}^p(t)dt = Q_{jp} \triangleq \int_0^\infty \phi^p f_j^*(\phi)d\phi\right\} = 1. \quad (2.2)$$

By direct calculation, we have

$$a_j = b_j Q_{j1} + \frac{\mu_j^2}{2} Q_{j2} \quad \text{when } a_j > 0. \quad (2.3)$$

The following two quantities play an important role in our analysis:

$$\begin{aligned} \lambda_1 &= a_2 + c_2 Q_{11} - \frac{\rho_2^2}{2} Q_{12} \quad \text{when } a_1 > 0, \\ \lambda_2 &= a_1 - c_1 Q_{21} - \frac{\rho_1^2}{2} Q_{22} \quad \text{when } a_2 > 0. \end{aligned}$$

We start with the case where the prey population has a negative intrinsic growth rate, and have the following result on the stochastic system (1.4) with $a_1 < 0$.

Theorem 2.1. (i) *If $a_1 < 0$ and $a_2 < 0$ then every solution $X_x(t)$ to (1.4) with initial value $x \in \mathbb{R}_+^{2,\circ}$ satisfies that almost surely $\lim_{t \rightarrow \infty} X_x(t) = (0, 0)$.*
(ii) *If $a_1 < 0 < a_2$ then every solution $X_x(t) = (X_{1,x}(t), X_{2,x}(t))$ to (1.4) with initial value $x \in \mathbb{R}_+^{2,\circ}$ satisfies that almost surely $\lim_{t \rightarrow \infty} X_{1,x}(t) = 0$ and the distribution of $X_{2,x}(t)$ converges weakly to π_2^* .*

As for the deterministic system associated with (1.4), we see that both prey and predator population die out when $a_1 < 0$ and $a_2 < 0$, and that the prey population goes extinct and predator tends to a_2/b_2 when $a_1 < 0 < a_2$. Comparing with the deterministic system associated with (1.4), Theorem 2.1 implies that the three white noises affect only the amplitude of the oscillation of sample paths instead of the long-time behavior of solutions to system (1.4) with $a_1 < 0$. In particular, the assumption that $a_1 < 0$ implies that almost surely $\lim_{t \rightarrow \infty} \psi_{1,x}(t) = 0$, and hence the density of the unique invariant probability measure of (2.1) is exactly the Dirac delta function $\delta(\cdot)$. In this case, λ_1 is actually equal to a_2 . As we shall see later, the sign of λ_1 determines whether the predator dies out or not.

Theorem 2.2. (i) *If $a_1 > 0 > a_2$ and $\lambda_1 < 0$ then every solution $X_x(t) = (X_{1,x}(t), X_{2,x}(t))$ to (1.4) with initial value $x \in \mathbb{R}_+^{2,\circ}$ satisfies that almost surely $\lim_{t \rightarrow \infty} X_{2,x}(t) = 0$ and $X_{1,x}(t)$ converges weakly to π_1^* .*
(ii) *If $a_1 > 0 > a_2$ and $\lambda_1 > 0$ then for any initial point $x \in \mathbb{R}_+^{2,\circ}$, system (1.4) is permanent, i.e., its solution $X_x(t)$ has a unique invariant probability concentrated on $\mathbb{R}_+^{2,\circ}$.*

It is easy to see that Theorem 2.2 unifies and improves the results obtained by Dang et al [5] who investigated the asymptotic behavior of system (1.3). As for the deterministic system associated with (1.4), we see that there exists a unique globally asymptotically stable (GAS) equilibrium $(a_1/b_1, 0)$ when $0 < a_1c_2 < -a_2b_1$, and that there exists a unique GAS equilibrium $((a_1b_2 - a_2c_1)/(b_1b_2 + c_1c_2), (a_1c_2 + a_2b_1)/(b_1b_2 + c_1c_2))$ when $a_1c_2 > -a_2b_1 > 0$. In particular, if $0 < a_1c_2 < -a_2b_1$, then it follows from (2.3) that

$$\lambda_1 < a_2 - \frac{a_2b_1}{a_1}Q_{11} - \frac{\rho_2^2}{2}Q_{12} = \frac{a_2\mu_1^2}{2a_1}Q_{12} - \frac{\rho_2^2}{2}Q_{12} < 0.$$

In view of Theorem 2.2(i), we obtain the following result.

Corollary 2.3. *Assume that $0 < a_1c_2 < -a_2b_1$, then every solution $X_x(t) = (X_{1,x}(t), X_{2,x}(t))$ to (1.4) with initial value $x \in \mathbb{R}_+^{2,\circ}$ satisfies that almost surely $\lim_{t \rightarrow \infty} X_{2,x}(t) = 0$, $X_{1,x}(t)$ converges weakly to π_1^* .*

The above corollary implies that if the predator population of the deterministic system associated with (1.4) dies out eventually, then the presence of noise in (1.4) cannot change this extinction tendency but either accelerate or delay the extinction of the predator population. However, if there is a stable coexisting equilibrium in the deterministic system associated with (1.4), then Theorem 2.2 implies that the presence of immoderate noise may cause the predator population to die out as well. This is exactly the essential difference between the stochastic system (1.4) and its deterministic system. This interesting observation can also be obtained in the case where $a_1 > 0$ and $a_2 > 0$. Namely, we have the following result.

Theorem 2.4. *Assume that $a_1 > 0$ and $a_2 > 0$.*

- (i) *If $\lambda_1 > 0$ and $\lambda_2 < 0$ then every solution $X_x(t) = (X_{1,x}(t), X_{2,x}(t))$ to (1.4) with initial value $x \in \mathbb{R}_+^{2,\circ}$ satisfies that almost surely $\limsup_{t \rightarrow \infty} X_{2,x}(t) > 0$, $\lim_{t \rightarrow \infty} X_{1,x}(t) = 0$ and $X_{2,x}(t)$ converges weakly to π_2^* .*
- (ii) *If $\lambda_1 < 0$ and $\lambda_2 > 0$ then every solution $X_x(t) = (X_{1,x}(t), X_{2,x}(t))$ to (1.4) with initial value $x \in \mathbb{R}_+^{2,\circ}$ satisfies that almost surely $\limsup_{t \rightarrow \infty} X_{1,x}(t) > 0$, $\lim_{t \rightarrow \infty} X_{2,x}(t) = 0$ and $X_{1,x}(t)$ converges weakly to π_1^* .*
- (iii) *If $\lambda_1 > 0$ and $\lambda_2 > 0$ then for any initial point $x \in \mathbb{R}_+^{2,\circ}$, then system (1.4) is permanent, i.e., its solution $X_x(t)$ has a unique invariant probability concentrated on $\mathbb{R}_+^{2,\circ}$.*

If $a_2 > 0$ and $\rho_2 = 0$ (i.e., there is no random influence on the inter-specific interaction term of prey population), then we have $\lambda_1 > 0$, which together with Theorem 2.4(i)(iii) implies the permanence of $X_{2,x}(t)$ for all $x \in \mathbb{R}_+^{2,\circ}$ and the existence of an invariant probability measure. Namely, we have the following result.

Corollary 2.5. *Assume that $a_1 > 0$, $a_2 > 0$, and $\rho_2 = 0$.*

- (i) *If $\lambda_2 < 0$ then every solution $X_x(t) = (X_{1,x}(t), X_{2,x}(t))$ to (1.4) with initial value $x \in \mathbb{R}_+^{2,\circ}$ satisfies that almost surely $\limsup_{t \rightarrow \infty} X_{2,x}(t) > 0$, $\lim_{t \rightarrow \infty} X_{1,x}(t) = 0$ and $X_{2,x}(t)$ converges weakly to π_2^* .*
- (ii) *If $\lambda_2 > 0$ then for any initial point $x \in \mathbb{R}_+^{2,\circ}$, then system (1.4) is permanent, i.e., its solution $X_x(t)$ has a unique invariant probability concentrated on $\mathbb{R}_+^{2,\circ}$.*

The dynamics of the deterministic system associated with (1.4) with $a_1 > 0$ and $a_2 > 0$ can be classified in terms of the sign of $a_1 b_2 - a_2 c_1$. In fact, the associated system has a unique GAS equilibrium $(0, a_2/b_2)$ when $0 < a_1 b_2 < a_2 c_1$, and has a unique GAS equilibrium $((a_1 b_2 - a_2 c_1)/(b_1 b_2 + c_1 c_2), (a_1 c_2 + a_2 b_1)/(b_1 b_2 + c_1 c_2))$ when $a_1 b_2 > a_2 c_1 > 0$. Even though the associated deterministic system is permanent, as we shall see, the presence of strong noises on the intra-specific interaction rate of the prey and predator may result in the extinction of the prey or predator population. On the other hand, even though the prey population of the associated deterministic system goes to extinction (for example, in the case where $0 < a_1 b_2 < a_2 c_1$), the stochastic system (1.4) may be permanent. In fact, we shall see in the subsequent numerical simulations that that strong noise on the intra-specific interaction rate of the predator population may lead to the permanence of the prey, which is different from the deterministic case.

Theorems 2.2 and 2.4 means that the signs of λ_1 and λ_2 determine the asymptotic behavior of the solution $X_x(t)$ to (1.4) with initial value $x \in \mathbb{R}_+^{2,\circ}$. A natural question is: what happens to the solution $X_x(t)$ when $\lambda_1 \lambda_2 = 0$? In fact, the set $\Xi = \{(a_1, a_2, b_1, b_2, c_1, c_2, \mu_1, \mu_2, \rho_1, \rho_2) \in \mathbb{R}^2 \times \mathbb{R}_+^{8,\circ} : \lambda_1 \lambda_2 = 0\}$ has Lebesgue measure 0 in the space $\mathbb{R}^2 \times \mathbb{R}_+^{8,\circ}$, and hence is negligible in the sense of the Lebesgue measure. Nevertheless, it is very interesting to explore the asymptotic behavior of the solution of (1.4) with parameters $(a_1, a_2, b_1, b_2, c_1, c_2, \mu_1, \mu_2, \rho_1, \rho_2) \in \Xi$. Unfortunately, this question remains open and we have to resort to new techniques. Finally, we do believe that our methods are applicable to stochastic predator-prey models with different types of functional response functions (i.e., replacing $X_1(t)X_2(t)$ of system (1.4) by some function of $X_1(t)$ and $X_2(t)$) (see [14, 15, 24, 31]) as well as to stochastic models with Markovian switching [12, 25].

3. NUMERICAL SIMULATIONS

To illustrate our theoretical results, we perform some numerical simulations of the solutions to (1.4), from which we find some interesting phenomena completely different from its corresponding deterministic system. By comparing the trajectories of the stochastic system (1.4) with those of the associated deterministic system, we clarify the effect of the intensity of each white noise on the dynamics of system (1.4) and provide some reasonable biological interpretation. As we shall see in Theorems 2.2 and 2.4, and Figures 9 and 13, different from the associated deterministic predator-prey system, strong noise on the intra-specific interaction rate of prey results in the extinction of the predator species even though the predator population persists in the associated deterministic system, while strong noise on the intra-specific interaction rate of the predator population may lead to the permanence of the prey even though the prey population dies out in the associated deterministic system. Furthermore, the population of the prey (or, predator) could decrease when there are strong noises on its corresponding intra-specific interaction rate, and strong noise on the inter-specific interaction rate of the prey population (or, the predator population) results in its extinction.

By applying Milstein scheme in [7], we have the following discretization system of model (1.4),

$$\begin{aligned} X_{k+1} &= X_k + X_k (a_1 - b_1 X_k - c_1 Y_k) \Delta t + X_k^2 [\mu_1 \xi_{1,k} \sqrt{\Delta t} + \frac{1}{2} \mu_1^2 (\xi_{1,k}^2 - 1) \Delta t] \\ &\quad + X_k Y_k [\rho_1 \xi_{3,k} \sqrt{\Delta t} + \frac{1}{2} \rho_1^2 (\xi_{3,k}^2 - 1) \Delta t], \\ Y_{k+1} &= Y_k + Y_k (a_2 - b_2 Y_k + c_2 X_k) \Delta t + Y_k^2 [\mu_2 \xi_{2,k} \sqrt{\Delta t} + \frac{1}{2} \mu_2^2 (\xi_{2,k}^2 - 1) \Delta t] \\ &\quad + X_k Y_k [\rho_2 \xi_{3,k} \sqrt{\Delta t} + \frac{1}{2} \rho_2^2 (\xi_{3,k}^2 - 1) \Delta t], \end{aligned}$$

where Δt is the time increment and $\xi_{1,k}$, $\xi_{2,k}$ and $\xi_{3,k}$ ($k = 1, 2, 3, \dots$) are independent Gaussian random variables which follow the standard Normal distribution $N(0, 1)$.

We first illustrate Theorem 2.1 by the stochastic systems

$$\begin{aligned} dX_t &= X_t(-0.1 - 0.3X_t - 0.25Y_t)dt + 0.1X_t^2 dW_1(t) + 0.1X_t Y_t dW_3(t), \\ dY_t &= Y_t(-0.1 - 0.25Y_t + 0.1X_t)dt + 0.1Y_t^2 dW_2(t) + 0.1X_t Y_t dW_3(t), \end{aligned} \quad (3.1)$$

and

$$\begin{aligned} dX_t &= X_t(-0.1 - 0.3X_t - 0.25Y_t)dt + \mu_1 X_t^2 dW_1(t) + \rho_1 X_t Y_t dW_3(t), \\ dY_t &= Y_t(0.2 - 0.25Y_t + 0.1X_t)dt + \mu_2 Y_t^2 dW_2(t) + \rho_2 X_t Y_t dW_3(t). \end{aligned} \quad (3.2)$$

It is easy to see that the deterministic system associated with (3.1) has a unique GAS equilibrium $(0, 0)$, and that the deterministic system associated with (3.2) has a unique GAS equilibrium $(0, 4/5)$. Obviously, Theorem 2.1(i) is illustrated by Figure 1, from which we see that both the prey and predator population go to extinction very fast and that the three white noises have no effect on sample paths of system (3.1). If the intensities of the three white noises is moderate, for example, $\mu_1 = \mu_2 = \rho_1 = \rho_2 = 0.1$, then the solution X_t of system (3.2) goes to zero while the solution Y_t oscillates around the value $\frac{4}{5}$ after some initial transients and the distribution of Y_t converges weakly to π_2^* (see Figure 2). In fact, we can

see that the larger the intensities of the white noises are, the larger the fluctuations of the solution Y_t will be. However, too large intensity μ_2 will make the solution Y_t become more close to zero while too large intensity ρ_1 will make the solution X_t vanish more rapidly (see Figures 3 and 4).

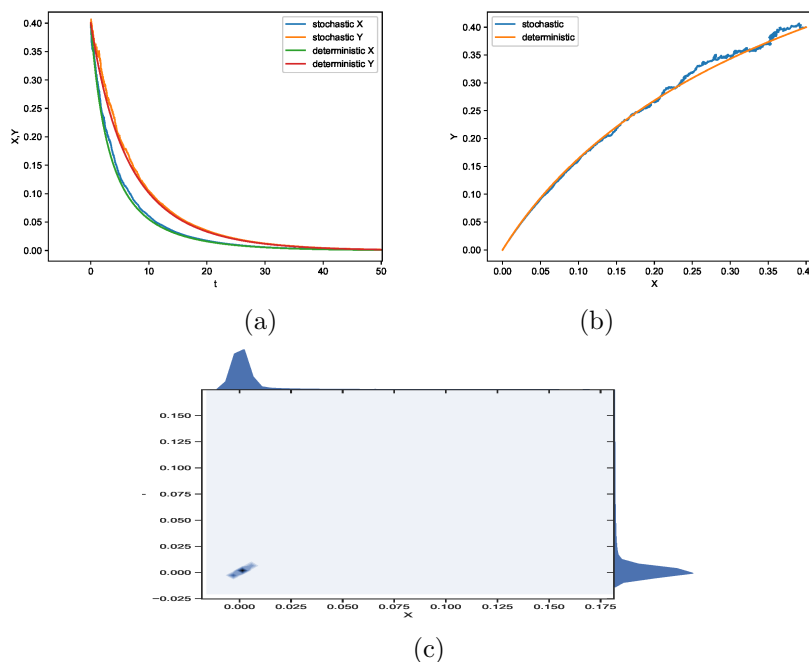


FIGURE 1. Numerical solutions to (3.1) with initial value $(X_0, Y_0) = (0.4, 0.4)$: (a) trajectories of solutions; (b) phase portrait; (c) top, right and inside of the box are the marginal and joint density distribution of solution (X, Y) , respectively.

We next consider the stochastic system

$$\begin{aligned} dX_t &= X_t(0.2 - 0.3X_t - 0.25Y_t)dt + \mu_1 X_t^2 dW_1(t) + \rho_1 X_t Y_t dW_3(t), \\ dY_t &= Y_t(-0.1 - 0.25Y_t + 0.1X_t)dt + \mu_2 Y_t^2 dW_2(t) + \rho_2 X_t Y_t dW_3(t), \end{aligned} \tag{3.3}$$

whose associated deterministic system has a unique GAS equilibrium $(\frac{2}{3}, 0)$. We first consider system (3.3) with parameters $\mu_1 = \mu_2 = \rho_1 = \rho_2 = 0.1$. An easy calculation yields that $\lambda_1 \approx -0.0363$. Figure 5 shows that the solution of model (3.3) oscillates around the deterministic equilibrium $(\frac{2}{3}, 0)$ after some initial transients, that is, Y_t goes to extinction and X_t weakly converges to π_1^* , which illustrates Theorem 2.2(i) and Corollary 2.3 as well. We also observe that increasing the intensity μ_2 or ρ_1 has little influence on the dynamical behaviours of (X, Y) of (3.3). Fix the intensities $\mu_2 = \rho_1 = \rho_2 = 0.1$ and increase the intensity μ_1 from 0.1 to 1, or fix the intensities $\mu_1 = \mu_2 = \rho_1 = 0.1$ and increase the intensity ρ_2 from 0.1 to 1, then we have $\lambda_1 \approx -0.0647$ and $\lambda_1 \approx -0.2538$, respectively. This, together with Theorem 2.2(i), implies that the predator population dies out. This theoretical result

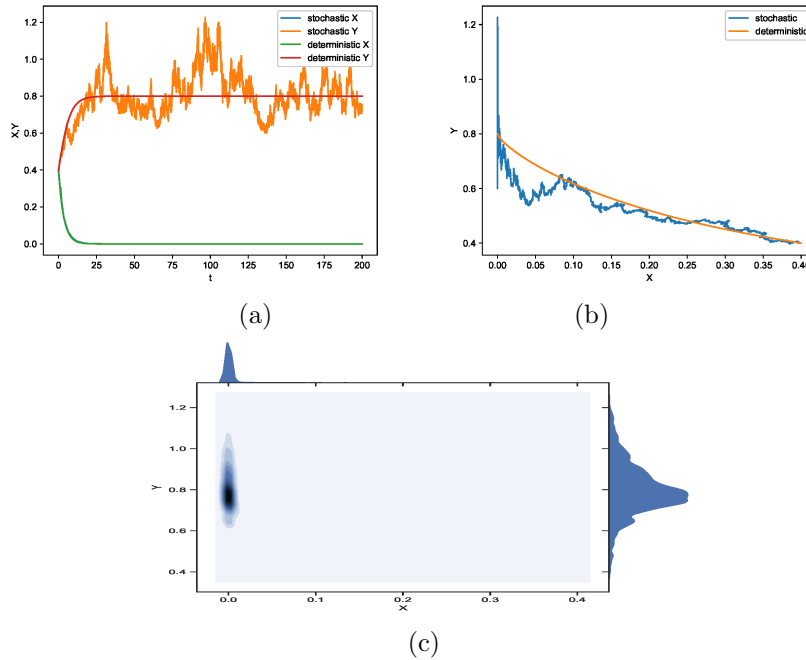


FIGURE 2. Numerical solutions to (3.2) with initial value $(X_0, Y_0) = (0.4, 0.4)$: (a) trajectories of solutions; (b) phase portrait; (c) top, right and inside of the box are the marginal and joint density distribution of solution (X, Y) , respectively.

is illustrated by Figures 6 and 7, from which we can see that Y_t goes to extinction faster if ρ_2 becomes larger.

Now we consider the stochastic system

$$\begin{aligned} dX_t &= X_t(0.37 - 0.3X_t - 0.25Y_t)dt + \mu_1 X_t^2 dW_1(t) + \rho_1 X_t Y_t dW_3(t), \\ dY_t &= Y_t(-0.1 - 0.25Y_t + 0.24X_t)dt + \mu_2 Y_t^2 dW_2(t) + \rho_2 X_t Y_t dW_3(t), \end{aligned} \quad (3.4)$$

whose associated deterministic system has a unique GAS equilibrium $(\frac{47}{54}, \frac{98}{225})$. We first consider system (3.4) with parameters $\mu_1 = \mu_2 = \rho_1 = \rho_2 = 0.1$. Direct calculation yields $\lambda_1 \approx 0.1826$. This, together with Theorem 2.2(ii) implies that the two species (X, Y) coexist. This theoretical result is illustrated by Figure 8, from which we can see that the solution of model (3.4) oscillates around the deterministic equilibrium $(47/54, 98/225)$ after some initial transients. We also observe that the increase of the intensity of μ_2 and ρ_1 has no much influence on the dynamical behaviours of solutions X_t and Y_t of (3.4). Fix the intensities $\mu_2 = \rho_1 = \rho_2 = 0.1$ and increase μ_1 from 0.1 to 2 (see Figure 9), or fix $\mu_1 = \mu_2 = \rho_1 = 0.1$ and increase ρ_2 from 0.1 to 1 (see Figure 10), then we have $\lambda_1 = -0.0277$ and $\lambda_1 = -0.5552$, respectively. This, together with Theorem 2.2(i), implies that Y_t goes to extinction and X_t weakly converges to a boundary distribution π_1^* . Indeed, we can find out that the larger intensities μ_1 and/or ρ_2 , the faster the convergence of Y_t to 0, which means that strong noise whether on the intra-specific interaction rate of prey or

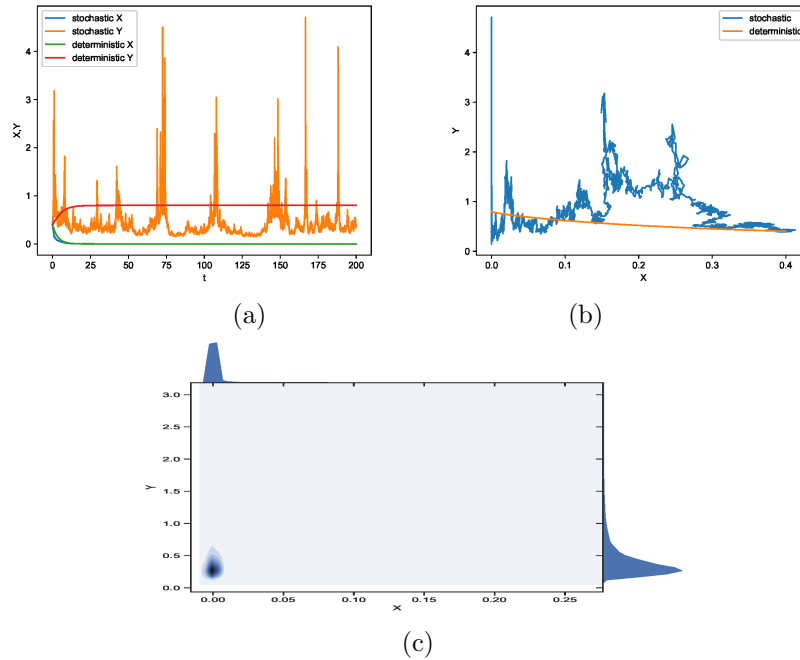


FIGURE 3. Numerical solutions to (3.2) with initial value $(X_0, Y_0) = (0.4, 0.4)$ and parameters $\mu_1 = \rho_1 = \rho_2 = 0.1$ and $\mu_2 = 1$: (a) trajectories of solutions; (b) phase portrait; (c) top, right and inside of the box are the marginal and joint density distribution of solution (X, Y) , respectively.

inter-specific interaction rate of predator results in the extinction of the predator species.

Now we consider the stochastic system

$$\begin{aligned} dX_t &= X_t(0.2 - 0.6X_t - 0.35Y_t)dt + \mu_1 X_t^2 dW_1(t) + \rho_1 X_t Y_t dW_3(t), \\ dY_t &= Y_t(0.5 - 0.5Y_t + 0.3X_t)dt + \mu_2 Y_t^2 dW_2(t) + \rho_2 X_t Y_t dW_3(t), \end{aligned} \quad (3.5)$$

whose associated deterministic system has a unique GAS equilibrium $(0, 1)$. First, we choose the following parameters $\mu_1 = \mu_2 = \rho_1 = \rho_2 = 0.1$. An easy calculation yields $\lambda_1 \approx 0.5$ and $\lambda_2 \approx -0.1515$, which together with Theorem 2.4 implies that X_t goes to extinction and Y_t converges to a boundary distribution π_2^* . From Figure 11 we can see that the solution of model (3.5) oscillates around the deterministic equilibrium $(0, 1)$ after some initial transients. To find out the effect of intensity of noises on the dynamical behaviours of X_t and Y_t , we shall increase the intensity μ_1 , μ_2 , ρ_1 and ρ_2 , respectively. If we increase the intensities μ_1 and ρ_2 , respectively, there is nothing new about the trajectories of X_t and Y_t . If we fix $\mu_1 = \mu_2 = \rho_2 = 0.1$ and increase intensity ρ_1 from 0.1 to 1, we have $\lambda_1 \approx 0.5$ and $\lambda_2 \approx -0.6416$ and find that X_t converges to 0 faster (see Figure 12). This means that strong intensity of noise on the inter-specific interaction rate of the prey leads to a faster speed of extinction of the prey. Next, fix $\mu_1 = \rho_1 = \rho_2 = 0.1$ and increase μ_2 from 0.1 to

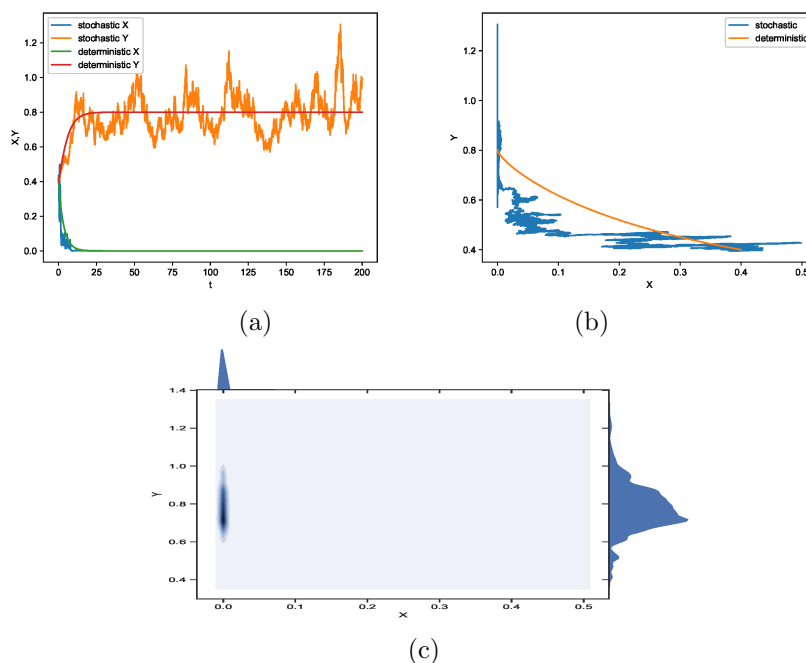


FIGURE 4. Numerical solutions to (3.2) with initial value $(X_0, Y_0) = (0.4, 0.4)$ and parameters $\mu_1 = \mu_2 = \rho_2 = 0.1$ and $\rho_1 = 2$: (a) trajectories of solutions; (b) phase portrait; (c) top, right and inside of the box are the marginal and joint density distribution of solution (X, Y) , respectively.

2, then we have $\lambda_2 \approx 0.0818$ and $\lambda_1 \approx 0.5$. Figure 13 shows that X_t is away from 0 and (X_t, Y_t) coexist, which further illustrate Theorem 2.4(iii). This implies that strong noise on the intra-specific interaction rate of the predator population may lead to the permanence of the prey which is different from the deterministic case.

Finally, we consider the system

$$\begin{aligned} dX_t &= X_t(0.8 - 0.6X_t - 0.35Y_t)dt + \mu_1 X_t^2 dW_1(t) + \rho_1 X_t Y_t dW_3(t), \\ dY_t &= Y_t(0.5 - 0.5Y_t + 0.3X_t)dt + \mu_2 Y_t^2 dW_2(t) + \rho_2 X_t Y_t dW_3(t), \end{aligned} \quad (3.6)$$

whose associated deterministic system has a unique GAS endemic equilibrium $(5/9, 4/3)$. For the parameters $\mu_1 = \mu_2 = \rho_1 = \rho_2 = 0.1$, we have $\lambda_2 \approx 0.4485$ and $\lambda_1 \approx 0.8868$. This, together with Theorem 2.4(iii), implies that the two species (X_t, Y_t) coexist. This theoretical result is illustrated by Figure 14, from which we can see that the solution of model (3.6) oscillates around the deterministic equilibrium $(5/9, 4/3)$.

We next study the effect of intensities of noises on the dynamical behaviours of (3.6). Fix $\mu_2 = \rho_1 = \rho_2 = 0.1$ and increase μ_1 from 0.1 to 1.1, then we have $\lambda_2 \approx 0.4485$ and $\lambda_1 \approx 0.7005$. From Figure 15, we see that the two species coexist, but the solution X_t becomes closer to 0 and the probability distribution of the solution of Y_t becomes closer to the invariant measure π_2^* . Fix $\mu_1 = \rho_1 = \rho_2 =$

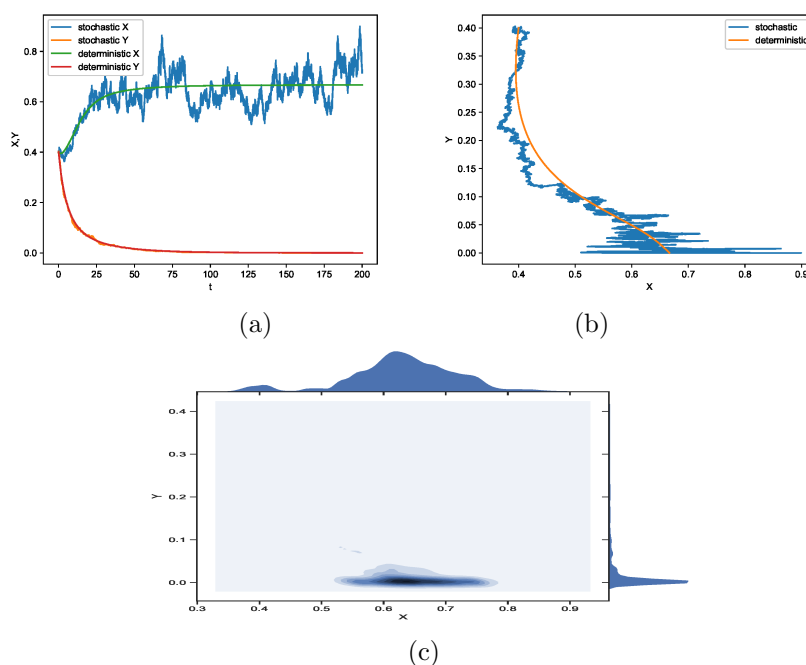


FIGURE 5. Numerical solutions to (3.3) with initial value $(X_0, Y_0) = (0.4, 0.4)$ and parameters $\mu_1 = \mu_2 = \rho_1 = \rho_2 = 0.1$: (a) Trajectories of solutions; (b) phase portrait; (c) top, right and inside of the box are the marginal and joint density distribution of solution (X, Y) , respectively.

0.1 and increase μ_2 from 0.1 to 1, then we also observe that (X, Y) coexists but the solution X_t is closer to the trajectories of $\varphi_x(t)$ and the solution Y_t is closer to 0 (see Figure 16). This implies that the population of the prey and predator could decrease when there are strong noises on their corresponding intra-specific interaction rate, respectively. Increasing the intensity ρ_1 from 0.1 to 1 while fixing $\mu_1 = \mu_2 = \rho_2 = 0.1$, we have $\lambda_1 \approx 0.8868$ and $\lambda_2 \approx -0.0416$, which satisfies the assumption of Theorem 2.4(i). In fact, we see from Figure 17 that the solution X_t is eventually extinct. As we increase the intensity ρ_1 further, the solution X_t converges to 0 faster. In this case, strong noise on the inter-specific interaction rate of the prey population results in the extinction of the prey species. Similarly, increasing the intensity ρ_2 from 0.1 to 1.1 while fixing $\mu_1 = \mu_2 = \rho_1 = 0.1$, we have $\lambda_1 \approx -0.1681$ and $\lambda_2 \approx 0.4485$, which together with Theorem 2.4(ii) implies that the solution Y_t goes to extinction. This theoretical result is illustrated by Figure 18. As we increase intensity ρ_2 further, Y_t converges to 0 faster. We see that strong noise on the inter-specific interaction rate of the predator population leads to the extinction of the predator population .

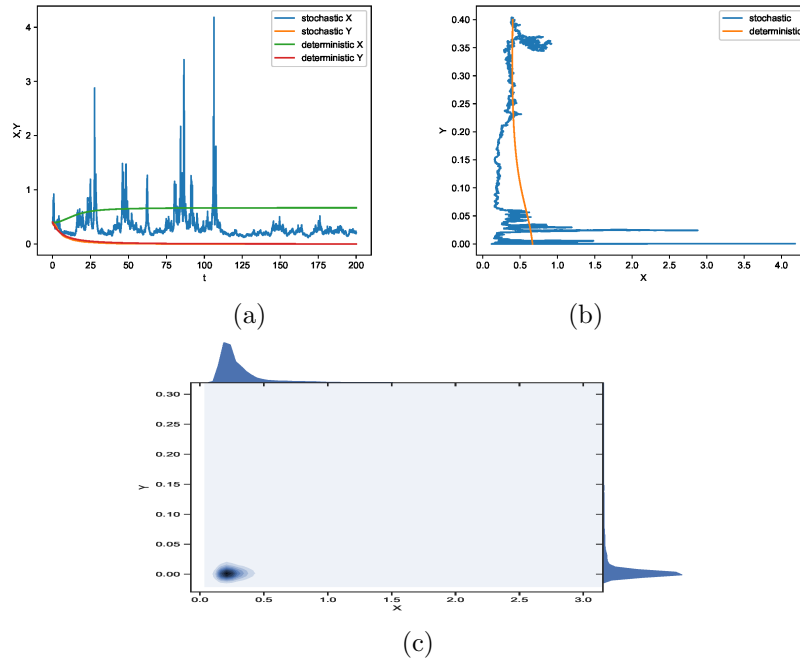


FIGURE 6. Numerical solutions to (3.3) with initial value $(X_0, Y_0) = (0.4, 0.4)$ and parameters $\mu_1 = 1$, $\mu_2 = \rho_1 = \rho_2 = 0.1$: (a) trajectories of solutions; (b) phase portrait; (c) top, right and inside of the box are the marginal and joint density distribution of solution (X, Y) , respectively.

4. PROOF OF THEOREM 2.1

Lemma 4.1 ([12, 20, 21]). *For every $p \in (0, 3)$, there exists a positive constant M_p such that $\mathbb{E} \int_0^t \|X_x(s)\|^p ds \leq M_p(t + \|x\|)$ for all $x \in \mathbb{R}_+^{2,0}$ and $t \geq 0$.*

Note that

$$\mathbb{E} \left| \int_0^T \mu_j X_{j,x}(t) dW_j(t) + \rho_j X_{3-j,x}(t) dW_3(t) \right|^2 = \mathbb{E} \int_0^T (\mu_j^2 X_{j,x}^2(t) + \rho_j^2 X_{3-j,x}^2(t)) dt,$$

then by Lemma 4.1 and Chebyshev's inequality, we see that for any $\varsigma > 0$, there exists a positive constant \widehat{M} such that

$$\mathbb{P} \left\{ \left| \int_0^T \mu_j X_{j,x}(t) dW_j(t) + \rho_j X_{3-j,x}(t) dW_3(t) \right| \leq \frac{\widehat{M}}{\varsigma} \sqrt{T \|z\|} \right\} \geq 1 - \varsigma. \quad (4.1)$$

We define the stopping time of $X_{j,x}$ as $\tau_{j,x}^\sigma = \inf\{t \geq 0 : X_{j,x}(t) \geq \sigma\}$, $j = 1, 2$. For $R > 1$ and $\delta > 0$, let

$$D_1^{R,\delta} = (0, \delta] \times [R^{-1}, R], \quad D_2^{R,\delta} = [R^{-1}, R] \times (0, \delta].$$

Then we have the following results.

Lemma 4.2. *For any $j = 1, 2$, $R > 1$, $T > 1$, $\varsigma > 0$ and $\sigma > 0$, there is a positive constant δ such that $\mathbb{P}\{\tau_{j,x}^\sigma \geq T\} \geq 1 - \varsigma$ for all $x \in D_j^{R,\delta}$.*

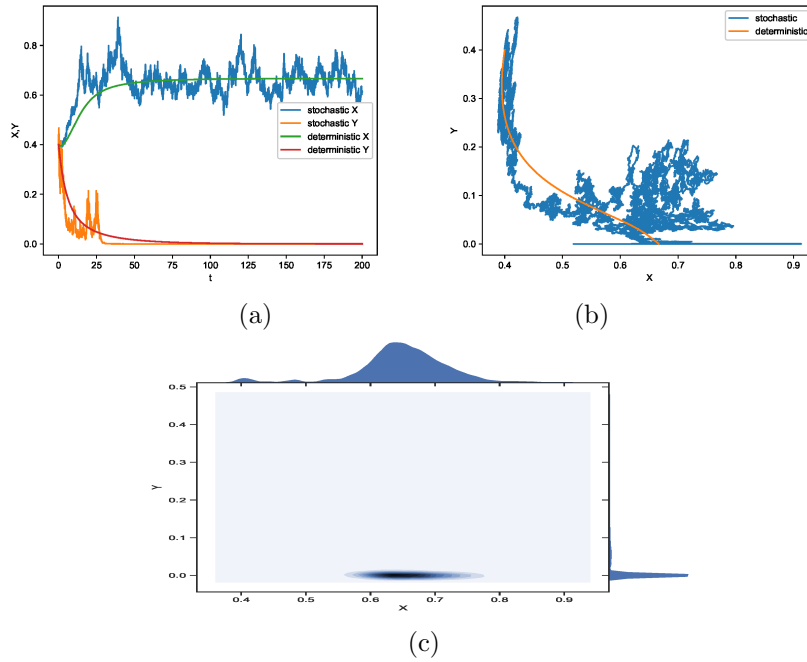


FIGURE 7. Numerical solutions to (3.3) with initial value $(X_0, Y_0) = (0.4, 0.4)$ and parameters $\mu_1 = \mu_2 = \rho_1 = 0.1, \rho_2 = 1$: (a) trajectories of solutions; (b) phase portrait; (c) top, right and inside of the box are the marginal and joint density distribution of solution (X, Y) , respectively.

The proof of the above lemma is similar to that in [23] and hence we omit it. The following result means that $X_{j,x}(t)$ is close to $\psi_{j,x}(t)$ if $X_{3-j,x}(t)$ is small for a sufficiently long time.

Lemma 4.3. *For any $j = 1, 2, R, T > 1$ and positive constants ς, ν , and γ , there exists a positive constant σ such that for all $x \in D_{3-j}^{R,\sigma}$,*

$$\mathbb{P}\{|\psi_{j,x}(t) - X_{j,x}(t)| < \nu \text{ and } |\Phi_{j,x}(t)| < \gamma \text{ for all } t \in [0, T \wedge \tau_{3-j,x}^\sigma]\} \geq 1 - \varsigma,$$

where $\Phi_{j,x}(t) = \frac{1}{\psi_{j,x}(t)} - \frac{1}{X_{j,x}(t)}$.

The proof of the above lemma is similar to that in [23] and hence we omit it.

Proof of Theorem 2.1(i). By exponential martingale inequality, we have $\mathbb{P}(\Omega_j^x) \geq 1 - \varsigma$, where

$$\begin{aligned} \Omega_j^x &= \left\{ \int_0^t (\mu_j X_{j,x}(s) dW_j(s) + \rho_j X_{3-j,x}(s) dW_3(s)) \right. \\ &\quad \left. \leq \ln \frac{1}{\varsigma} + \frac{1}{2} \int_0^t (\mu_j^2 X_{j,x}^2(s) + \rho_j^2 X_{3-j,x}^2(s)) ds \text{ for all } t \geq 0 \right\}, \quad j = 1, 2. \end{aligned}$$

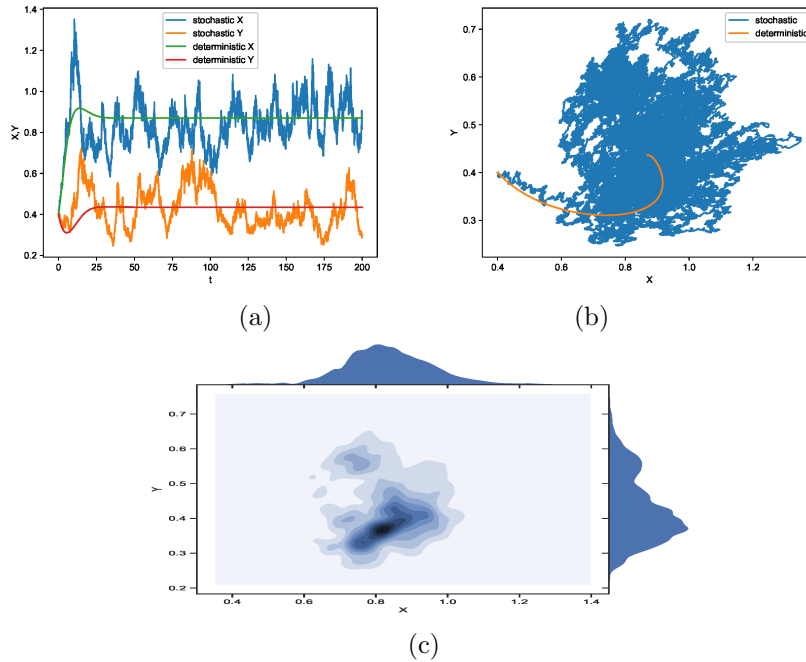


FIGURE 8. Numerical solutions to (3.4) with initial value $(X_0, Y_0) = (0.4, 0.4)$ and parameters $\mu_1 = \mu_2 = \rho_1 = \rho_2 = 0.1$: (a) trajectories of X and Y ; (b) phase portrait; (c) top, right and inside of the box are the marginal and joint density distribution of solution (X, Y) , respectively.

Applying Itô's formula to the first equation of (1.4) yields that for $\omega \in \Omega_1^x$ and $t > 0$, $\ln X_{1,x}(t) \leq \ln x + \ln \frac{1}{\zeta} + a_1 t$ and so

$$\limsup_{t \rightarrow \infty} \frac{1}{t} \ln X_{1,x}(t) \leq a_1, \tag{4.2}$$

which implies that almost surely

$$\lim_{t \rightarrow \infty} X_{1,x}(t) = 0, \quad \lim_{t \rightarrow \infty} \frac{1}{t} \int_0^t X_{1,x}(t) dt = 0. \tag{4.3}$$

Similarly, applying Itô's formula to the second equation of (1.4) yields that for $\omega \in \Omega_2^x$ and $t > 0$, we have

$$\ln X_{2,x}(t) \leq \ln x_2 + \ln \frac{1}{\zeta} + a_2 t + c_2 \int_0^t X_{1,x}(t) dt, \tag{4.4}$$

which together with (4.3) implies that almost surely $\lim_{t \rightarrow \infty} X_{2,x}(t) = 0$. The proof is complete. \square

Lemma 4.4. *Assume that $a_1 < 0 < a_2$, then for any $\zeta > 0$, $R > 1$, there are $T = T(\zeta, R) > 0$ and $\delta_0 = \delta_0(\zeta, R) > 0$ such that $\mathbb{P}(\tilde{\Omega}^x) > 1 - \zeta$ for all $x = (x_1, x_2) \in D_2^{R, \delta_0}$, where $\tilde{\Omega}^x = \{\ln X_{2,x}(T) - \ln x_2 \geq \frac{1}{4} a_2 T\}$. Moreover, there are*

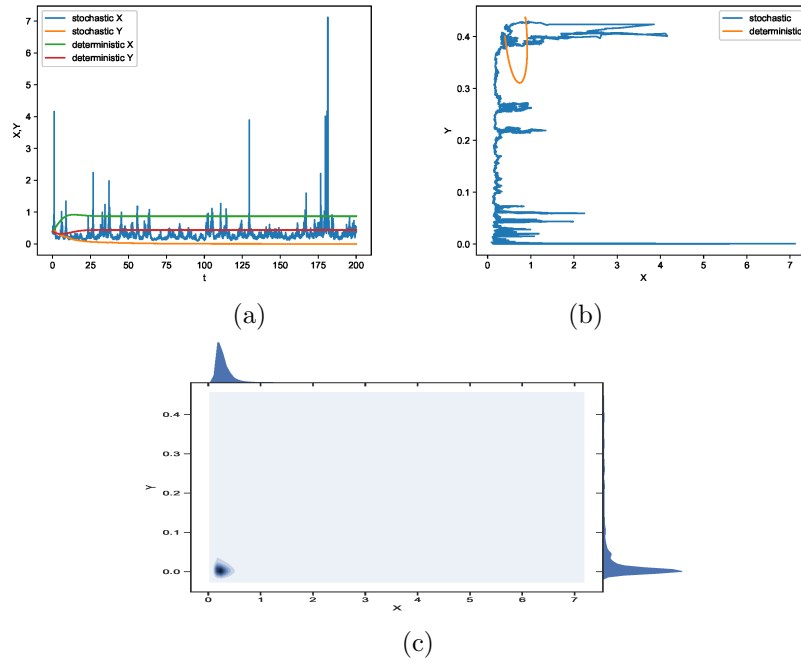


FIGURE 9. Numerical solutions to (3.4) with initial value $(X_0, Y_0) = (0.4, 0.4)$ and parameters $\mu_1 = 2, \mu_2 = \rho_1 = \rho_2 = 0.1$: (a) trajectories of solutions; (b) phase portrait; (c) top, right and inside of the box are the marginal and joint density distribution of solution (X, Y) , respectively.

$T = T(\varsigma)$ and $\delta_1 = \delta_1(\varsigma) > 0$ such that

$$\limsup_{N \rightarrow \infty} \frac{1}{N} \sum_{k=0}^{N-1} \mathbb{P}\{X_{2,x}(kT) \leq \delta_1\} \leq \varsigma \quad \text{for all } x \in \mathbb{R}_+^{2,\circ}. \tag{4.5}$$

Proof. As stated in the proof of Theorem 2.1(i), $\lim_{t \rightarrow \infty} X_{1,x}(t) = 0$ almost surely and hence for any given positive constant $\varsigma < a_2/(2\rho_2^2)$ there exists $T_1 > 0$ such that almost surely

$$X_{1,x}(t) < \varsigma, \quad \frac{1}{t} \int_0^t X_{1,x}(s) ds < \varsigma, \quad \frac{1}{t} \int_0^t X_{1,x}^2(s) ds < \varsigma$$

for all $t > T_1$. Choose $\sigma = \sigma(\varsigma, R) > 0$ such that $b_2\sigma + \frac{1}{2}\mu_2^2\sigma^2 \leq a_2/4$. Lemma 4.2 implies that there exists $\delta_0 = \delta_0(\varsigma, R) > 0$ such that $\mathbb{P}(\Omega_3^x) \geq 1 - \varsigma$ for all $x \in D_2^{R,\delta_0}$, where $\Omega_3^x = \{\tau_{2,x}^\sigma \geq T_1\}$. Let $T_2 > 16\widehat{M}^2R/(\varsigma^2a_2^2)$, then it follows from (4.1) that $\mathbb{P}(\Omega_4^x) \geq 1 - \varsigma$, where

$$\Omega_4^x = \left\{ \left| \int_0^{T_2} \mu_2 X_{2,x}(t) dW_2(t) + \rho_2 X_{1,x}(t) dW_3(t) \right| \leq \frac{1}{4} a_2 T_2 \right\}.$$

Let $T = T_1 \wedge T_2$, then applying Itô's formula to the second equation of (1.4) yields that $\ln X_{2,x}(T) - \ln x_2 \geq \frac{1}{4} a_2 T$ for $x \in D_2^{R,\delta_0}$ and $\omega \in \tilde{\Omega}^x = \Omega_3^x \cap \Omega_4^x$. Consequently,

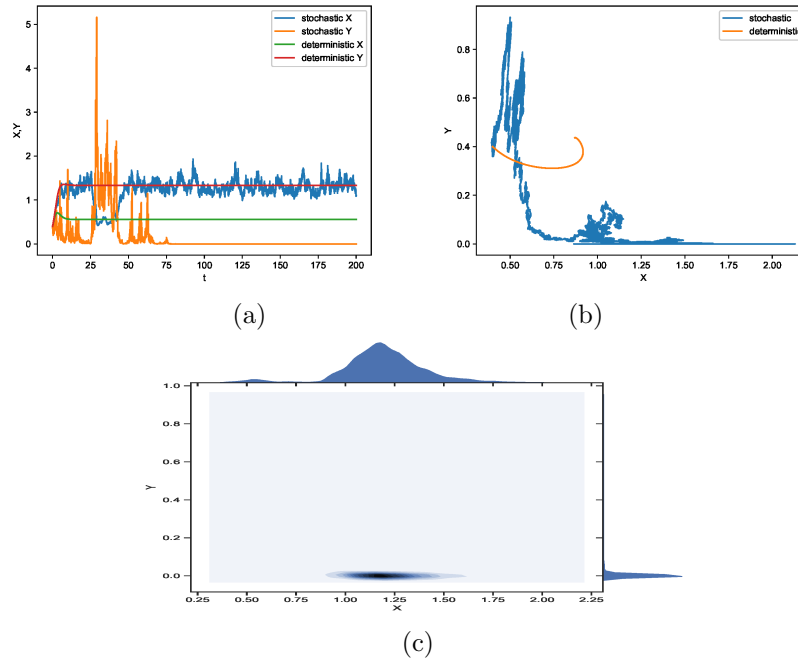


FIGURE 10. Numerical solutions to (3.4) with initial value $(X_0, Y_0) = (0.4, 0.4)$ and parameters $\rho_2 = 1, \mu_1 = \mu_2 = \rho_1 = 0.1$: (a) trajectories of solutions; (b) phase portrait; (c) top, right and inside of the box are the marginal and joint density distribution of solution (X, Y) , respectively.

we obtain $\mathbb{P}(\tilde{\Omega}^x) > 1 - \varsigma$. Similarly to [23, Proposition 3.2], we conclude that there are $T = T(\varsigma)$ and $\delta_1 = \delta_1(\varsigma) > 0$ such that (4.5) holds, which implies that $X_{2,x}$ is away from zero for all $x \in \mathbb{R}_+^{2,\circ}$. The proof is complete. \square

Proof of Theorem 2.1(ii). As in the proof of Theorem 2.1(i), $\lim_{t \rightarrow \infty} X_{1,x}(t) = 0$ almost surely. In view of (4.2), there exists a positive random variable C_1 such that $X_{1,x}(t) \leq C_1 \exp\{(a_1 + \epsilon)t\}$ for $t > 0$ and sufficiently small ϵ . It is easy to see that there exists $R > 1$ such that

$$\limsup_{t \rightarrow \infty} \mathbb{P}\{X_x(t) \in C\} \geq 1 - \varsigma, \tag{4.6}$$

where $C \triangleq \{R^{-1} \leq x_1 \vee x_2 \leq R\}$. Using a similar argument as the proof of [23, Proposition 4.1], there exists $\delta > 0$ such that $\mathbb{P}(\Omega_5^x) \geq 1 - \varsigma$ for all $x \in D_1^{R,\delta}$, where $\Omega_5^x = \{|\Phi_{2,x}(t)| \leq 1\}$. By Lemma 4.4, there exist $T > 1$ and $\delta_1 > 0$ such that

$$\limsup_{N \rightarrow \infty} \frac{1}{N} \sum_{i=0}^{N-1} \mathbb{P}\{X_{2,x}(iT) < \delta_1\} \leq \varsigma. \tag{4.7}$$

Note that $C_1 \triangleq C \setminus (D_1^{R,\delta} \cup \{(x_1, x_2) : x_2 < \delta_1\})$ is compact and that $X(t)$ is not recurrent in $\mathbb{R}_+^{2,\circ}$ (see [23, Proposition 4.1] for the related proof). Then

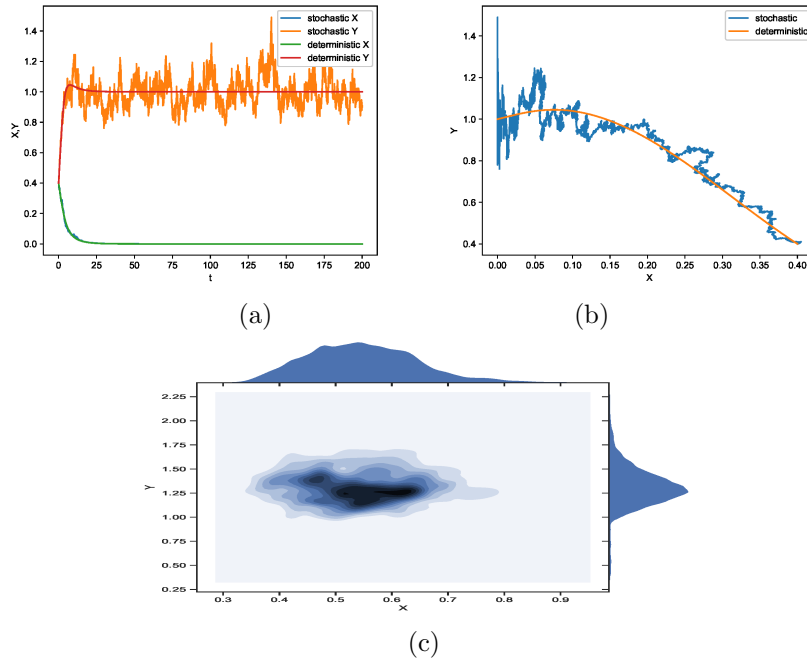


FIGURE 11. Numerical solutions to (3.5) with initial value $(X_0, Y_0) = (0.4, 0.4)$ and parameters $\mu_1 = \mu_2 = \rho_1 = \rho_2 = 0.1$: (a) Trajectories of solutions; (b) phase portrait; (c) top, right and inside of the box are the marginal and joint density distribution of solution (X, Y) , respectively.

the non-degeneracy of the diffusion implies that $X(t)$ is transient and hence that $\lim_{t \rightarrow \infty} \mathbb{P}\{X_x(t) \in C_1\} = 0$. This together with (4.6) and (4.7) implies that

$$\limsup_{N \rightarrow \infty} \frac{1}{N} \sum_{i=0}^{N-1} \mathbb{P}\{X_x(iT) \in D_1^{R,\delta}\} \geq 1 - 2\varsigma,$$

and hence that there exists i_0 such that $\mathbb{P}\{X_x(i_0T) \in D_1^{R,\delta}\} \geq 1 - 3\varsigma$, which together with Markov property implies that $\mathbb{P}\{|\Phi_{2,x}(t)| < 1\} \geq (1 - 3\varsigma)^2 \geq 1 - 6\varsigma$ for all $x \in \mathbb{R}_+^{2,\circ}$.

In what follows, we shall show that $X_{2,x}(t)$ converges to $\psi_{2,x}(t)$. It follows from Itô's formula that

$$\begin{aligned} d[e^{2\rho t} \Phi_{2,x}^2(t)] &= e^{2\rho t} h(\psi_{2,x}(t), X_{1,x}(t), X_{2,x}(t)) dt \\ &\quad + e^{2\rho t} g(\psi_{2,x}(t), X_{1,x}(t), X_{2,x}(t)) dW_3(t) + 2\rho e^{2\rho t} \Phi_{2,x}^2(t) \end{aligned}$$

where $\rho = \min\{a_2, -a_1 - \varsigma\}$ and

$$\begin{aligned} h(\psi, x, y) &= 2(c_2x - \rho_2^2x^2) \frac{1}{y} \left(\frac{1}{\psi} - \frac{1}{y}\right) + 2\mu_2^2(\psi - y) \left(\frac{1}{\psi} - \frac{1}{y}\right) \\ &\quad + \rho_2^2 \frac{x^2}{y^2} - 2a_2 \left(\frac{1}{\psi} - \frac{1}{y}\right)^2, \end{aligned}$$

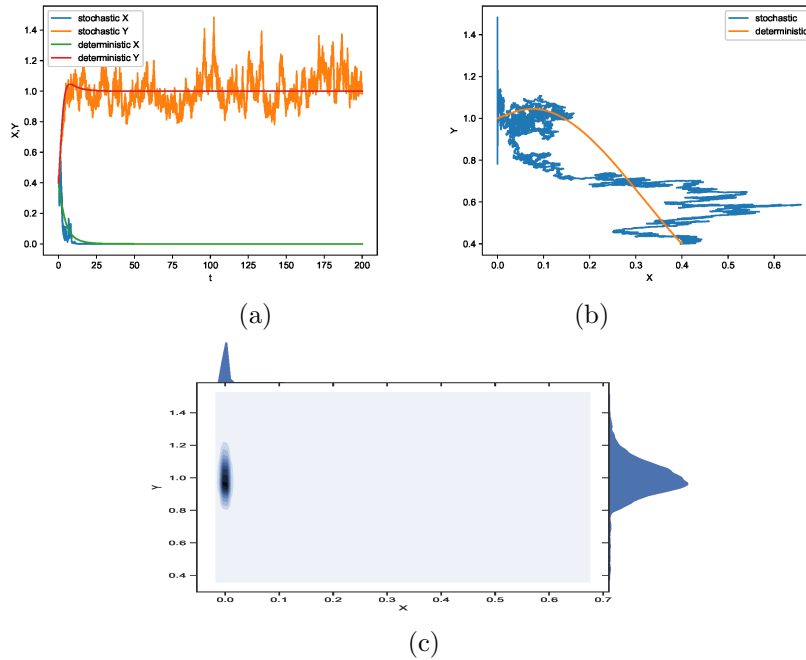


FIGURE 12. Numerical solutions to (3.5) with initial value $(X_0, Y_0) = (0.4, 0.4)$ and parameters $\mu_1 = \mu_2 = \rho_2 = 0.1$, $\rho_1 = 1$: (a) trajectories of solutions; (b) phase portrait; (c) top, right and inside of the box are the marginal and joint density distribution of solution (X, Y) , respectively.

$$g(\psi, x, y) = 2\rho_2 \frac{x}{y} \left(\frac{1}{\psi} - \frac{1}{y} \right).$$

For each $\gamma > 0$, we have $\mathbb{P}(\Omega_6^x) \geq 1 - \zeta$, where

$$\begin{aligned} \Omega_6^x &= \left\{ \int_0^t g(\psi_{2,x}(s), X_{1,x}(s), X_{2,x}(s)) dW_3(s) \right. \\ &\quad \left. \leq \gamma + m_\gamma \int_0^t g^2(\psi_{2,x}(s), X_{1,x}(s), X_{2,x}(s)) ds \right\} \end{aligned}$$

and $m_\gamma = \frac{2}{\gamma} \ln \frac{1}{\zeta}$. For $\omega \in \Omega_6^x$,

$$\begin{aligned} e^{2\rho t} \Phi_{2,x}^2(t) &\leq \gamma + \int_0^t e^{2\rho s} h(\psi_{2,x}(s), X_{1,x}(s), X_{2,x}(s)) ds \\ &\quad + m_\gamma \int_0^t e^{4\rho s} g^2(\psi_{2,x}(s), X_{1,x}(s), X_{2,x}(s)) ds. \end{aligned}$$

Thus for $\omega \in \Omega_5^x \cap \Omega_6^x$, $\tilde{\Psi}_x(t) = e^{2\rho t} \Phi_{2,x}^2(t)$ satisfies

$$\tilde{\Psi}_x(t) \leq \gamma + 5C_1^2 \rho_2^2 \int_0^t \exp\{2(a_1 + \epsilon)s\} \tilde{\Psi}_x(s) ds + C_1^2 \left(\rho_2^2 + \frac{c_2^2}{a_2} + 4m_\gamma \rho_2^2 \right) \int_0^t \frac{ds}{\psi_{2,x}^2(s)}$$

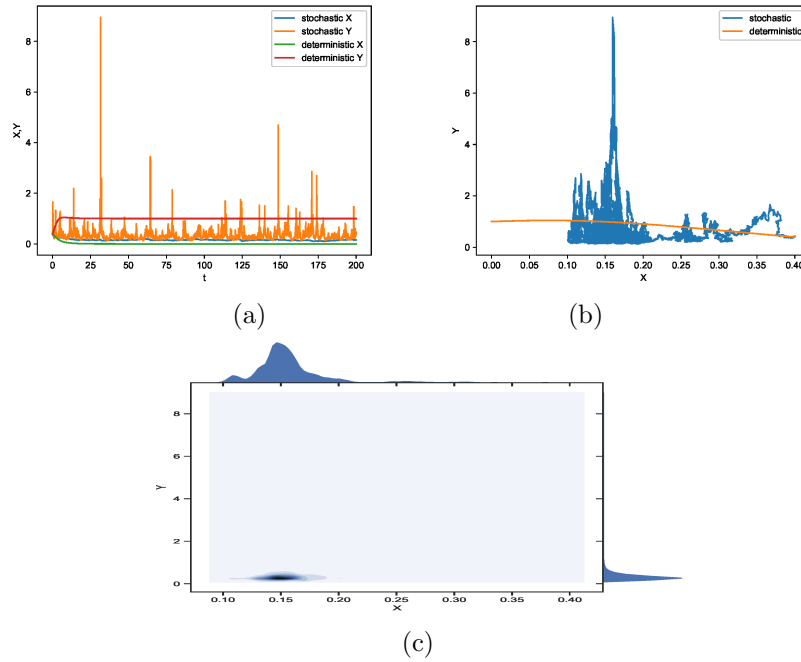


FIGURE 13. Numerical solutions to (3.5) with initial value $(X_0, Y_0) = (0.4, 0.4)$ and parameters $\mu_1 = \rho_1 = \rho_2 = 0.1, \mu_2 = 2$: (a) trajectories of solutions; (b) phase portrait; (c) top, right and inside are the marginal and joint density distribution of solution (X, Y) , respectively.

$$+ 4C_1^2 m_\gamma \rho_2^2 \int_0^t \tilde{\Psi}_x(s) \exp\{(2(\rho + a_1 + \epsilon)t\} ds.$$

In view of (2.2), there is $T = T(\varsigma, R) > 0$ such that $\mathbb{P}(\Omega_7^x) \geq 1 - \varsigma$ for all $x = (x_1, x_2)$ with $x_2 \in [R^{-1}, R]$, where

$$\Omega_7^x = \left\{ \frac{1}{t} \int_0^t \frac{ds}{\psi_{2,x}^2(s)} < 2Q_{2,-2}, t > T \right\}.$$

Thus, for all $\omega \in \Omega_5^x \cap \Omega_6^x \cap \Omega_7^x$ and $t > T$,

$$\tilde{\Psi}_x(t) \leq m_1(t) + \int_0^t m_2(s) \tilde{\Psi}_x(s) ds,$$

where

$$m_1(t) = \gamma + 2Q_{2,-2} C_1^2 \left(\rho_2^2 + \frac{c_2^2}{a_2} + 4m_\gamma \rho_2^2 \right) t,$$

$$m_2(t) = C_1^2 \rho_2^2 (5 + 4m_\gamma) \exp\{(2(\rho + a_1 + \epsilon)s)\}.$$

It follows from Gronwall's inequality that

$$\tilde{\Psi}_x(t) \leq m_1(t) + \int_0^t m_1(s) m_2(s) \exp \left\{ \int_s^t m_2(r) dr \right\} ds$$

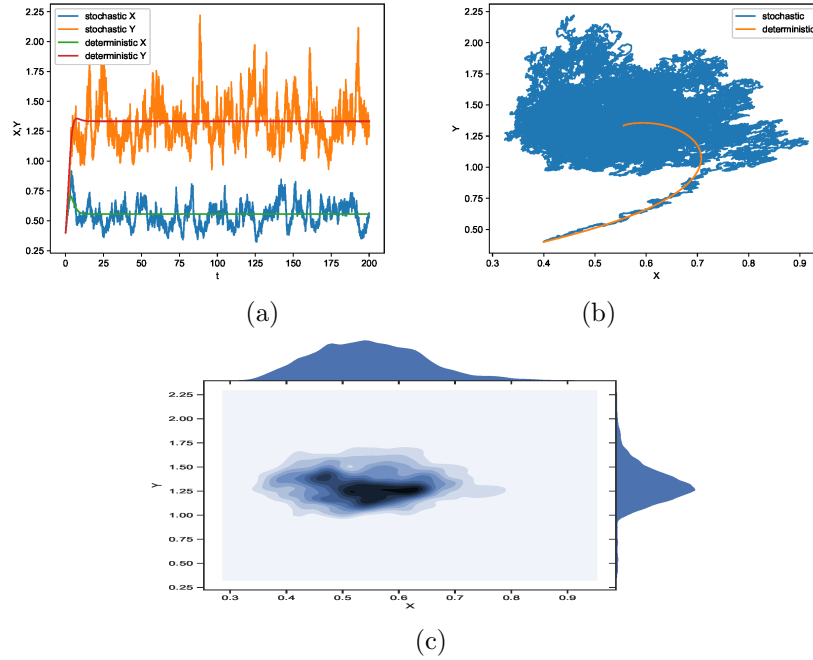


FIGURE 14. Numerics of solutions to (3.6) with initial value $(X_0, Y_0) = (0.4, 0.4)$ and parameters $\mu_1 = \mu_2 = \rho_1 = \rho_2 = 0.1$: (a) trajectories of X and Y ; (b) phase portrait; (c) top, right and inside of the box are the marginal and joint density distribution of solution (X, Y) , respectively.

for all $\omega \in \Omega_5^x \cap \Omega_6^x \cap \Omega_7^x$ and $t > T$, and hence that almost surely

$$\lim_{t \rightarrow \infty} \Phi_{2,x}^2(t) \leq \lim_{t \rightarrow \infty} e^{-2\rho t} \left[m_1(t) + \int_0^t m_1(s) m_2(s) \exp \left\{ \int_s^t m_2(r) dr \right\} ds \right] = 0.$$

The proof is complete. \square

5. PROOF OF THEOREM 2.2

This section is devoted to the case where the prey population has a positive intrinsic growth rate while the predator population has a negative intrinsic growth rate, that is, $a_1 > 0 > a_2$. We have the following result.

Lemma 5.1. *Assume that $a_1 > 0$ and $\lambda_1 < 0$, then for any $R > 1$, $\varsigma, \gamma' > 0$, there exists $\tilde{\delta} > 0$ such that for all $x \in D_2^{R, \tilde{\delta}}$,*

$$\mathbb{P} \left\{ \limsup_{t \rightarrow \infty} \frac{1}{t} \ln X_{2,x}(t) < 0 \text{ and } |\Phi_{1,x}(t)| < \gamma' \right\} \geq 1 - 3\varsigma.$$

Proof. Note that for each $R > 1$, there is $\bar{R} = \bar{R}(\epsilon, R, T) > 1$ such that $\mathbb{P}\{\bar{R}^{-1} \leq X_{1,x}(t) \leq \bar{R} \text{ for all } t \in [0, T]\} \geq 1 - \epsilon$ if $x \in [R^{-1}, R] \times [0, R]$. By Lemma 4.3, for any $R, T > 1$, $\varsigma, \gamma' > 0$, there exists $\tilde{\sigma} > 0$ such that $\mathbb{P}\{|\Phi_{1,x}(t)| < \gamma' \text{ for all } t \in [t, T \wedge t\tilde{\sigma}]\} \geq 1 - \varsigma$ for all $x \in D_2^{R, \tilde{\sigma}}$. Set $F(x, y) = -c_2(x + y) + \frac{1}{2}\rho_2^2(x - y)^2$.

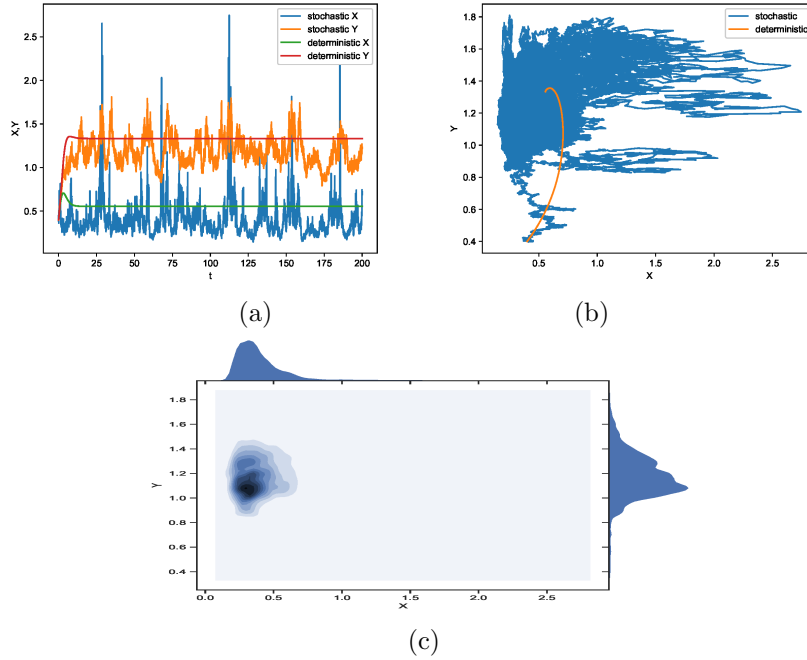


FIGURE 15. Numerical solutions to (3.6) with initial value $(X_0, Y_0) = (0.4, 0.4)$ and parameters $\mu_1 = 1.1, \mu_2 = \rho_1 = \rho_2 = 0.1$: (a) trajectories of solutions; (b) phase portrait; (c) top, right and inside of the box are the marginal and joint density distribution of solution (X, Y) , respectively.

Choose $\lambda \in (0, -\lambda_1)$ and $\vartheta \in (\frac{\lambda}{2}, -\frac{\lambda_1}{2})$. Since $\int_0^\infty F(\phi, 0)f_1^*(\phi)d\phi = a_2 - \lambda_1 < \infty$, we can find $\kappa_1, \kappa_2 \in (0, 1)$ and $d > 0$ such that

$$\int_{\kappa_1}^\infty F(\phi, \kappa_1)f_1^*(\phi)d\phi \geq a_2 - \lambda_1 - \vartheta = a_2 + \lambda + 3d,$$

$$\int_{\kappa_2^{-1}}^\infty F(\phi, \kappa_1)f_1^*(\phi)d\phi \leq d.$$

There exists $T_2 = T_2(\varsigma, R)$ such that for all $s \geq 0, x \in [R^{-1}, R] \times [0, R]$ and $t \geq T_2$,

$$\mathbb{P}\left\{\frac{1}{t} \int_0^t \mathbf{1}_{\{\kappa_1 \leq \psi_{1,x}(s)\}} F(\psi_{1,x}(s), \kappa_1) ds - (a_2 + \lambda) \geq 2d\right.$$

$$\left. \geq \frac{1}{t} \int_0^t \mathbf{1}_{\{\kappa_2^{-1} \leq \psi_{1,x}(s)\}} F(\psi_{1,x}(s), \kappa_1) ds\right\} > 1 - \varsigma,$$

and hence $\mathbb{P}(\Omega_8^x) \geq 1 - \varsigma$, where

$$\Omega_8^x = \left\{ a_2 - \frac{1}{t} \int_0^t \mathbf{1}_{\{\kappa_1 \leq \psi_{1,x}(s) \leq \kappa_2^{-1}\}} F(\psi_{1,x}(s), \kappa_1) ds \leq -\lambda \text{ for all } t \geq T_2 \right\}.$$

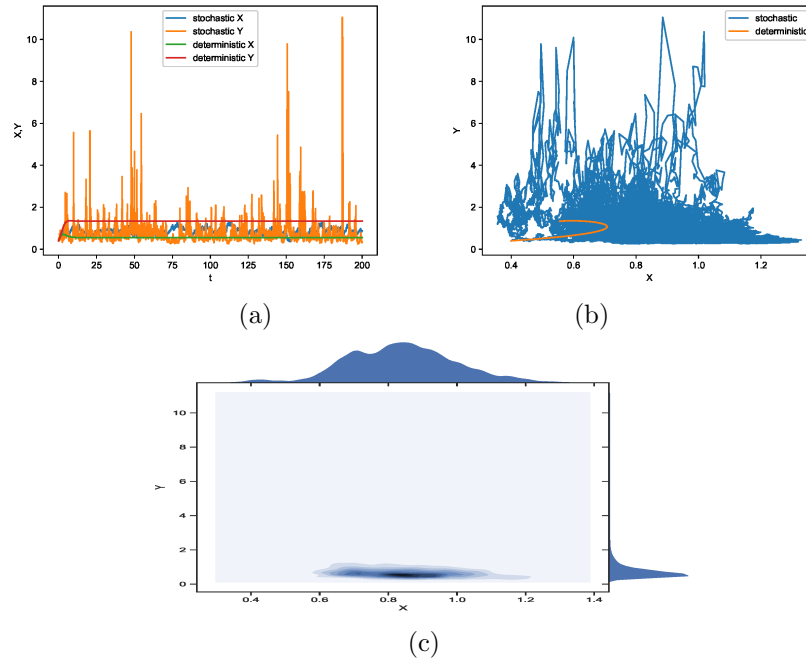


FIGURE 16. Numerical solutions to (3.6) with initial value $(X_0, Y_0) = (0.4, 0.4)$ and parameters $\mu_2 = 1$, $\mu_1 = \rho_1 = \rho_2 = 0.1$: (a) trajectories of solutions; (b) phase portrait; (c) top, right and inside of the box are the marginal and joint density distribution of solution (X, Y) , respectively.

Hence, for $\omega \in \Omega_8^x \cap \{\vartheta_x \geq T_2\}$, we have

$$\frac{1}{t} \int_0^t \left(a_2 + c_2 X_{1,x}(s) - \frac{\rho_2^2}{2} X_{1,x}^2(s) \right) ds \leq -\lambda \quad (5.1)$$

for all $t \in [T_2, \vartheta_x]$, where $\vartheta_x = \inf\{t > 0 : |\Phi_{1,x}(t)| \geq \gamma' \wedge (\kappa_1 \kappa_2^2)\}$. In view of (5.1), for $\omega \in \Omega_1^x \cap \Omega_8^x \cap \{\vartheta_x \geq T_2\}$, we have $\ln X_{2,x}(t) \leq \ln x_2 + \ln \frac{1}{\zeta} - \lambda t$ for all $t \in [T_2, \vartheta_x]$, which together with Lemma 4.2 implies that there exists $\tilde{\delta} = \tilde{\delta}(\zeta, R)$ so small that $\ln \tilde{\delta} + \ln \frac{1}{\zeta} - \lambda T_2 < \ln \tilde{\sigma}$ and $\mathbb{P}(\Omega_9^x) \geq 1 - \zeta$ for all $x \in D_2^{R, \tilde{\delta}}$, where $\Omega_9^x = \{\zeta_x \triangleq \vartheta_x \wedge \tau_{2,x}^{\tilde{\sigma}} \geq T_2\}$. Consequently, $\mathbb{P}(\tilde{\Omega}^x) \geq 1 - 3\zeta$, where $\tilde{\Omega}^x = \Omega_1^x \cap \Omega_8^x \cap \Omega_9^x$. As a result, for all $x \in D_2^{R, \tilde{\delta}}$ and $\omega \in \tilde{\Omega}^x$, we have

$$\ln X_{2,x}(t \wedge \tau_{2,x}^{\tilde{\sigma}}) \leq \ln x_2 + \ln \frac{1}{\zeta} - \lambda(t \wedge \tau_{2,x}^{\tilde{\sigma}}) < \ln \tilde{\sigma} \quad \text{for all } t \geq T_2.$$

and so $t \wedge \tau_{2,x}^{\tilde{\sigma}} < \tau_{2,x}^{\tilde{\sigma}}$ for all $t \geq T_2$, $x \in D_2^{R, \tilde{\delta}}$ and $\omega \in \tilde{\Omega}^x$, which means that $\tau_{2,x}^{\tilde{\sigma}} = \vartheta_x = \infty$ for all $x \in D_2^{R, \tilde{\delta}}$ and $\omega \in \tilde{\Omega}^x$. The proof is complete. \square

Lemma 5.2. *If $a_1 > 0 > a_2$ and $\lambda_1 < 0$, then for any $R > 1$, $\zeta > 0$, there exists $\delta > 0$ and $T = T(\zeta, R) > 0$ such that $\mathbb{P}(\tilde{\Omega}_x) = 1 - \zeta$ for all $x \in D_1^{R, \delta}$, where*

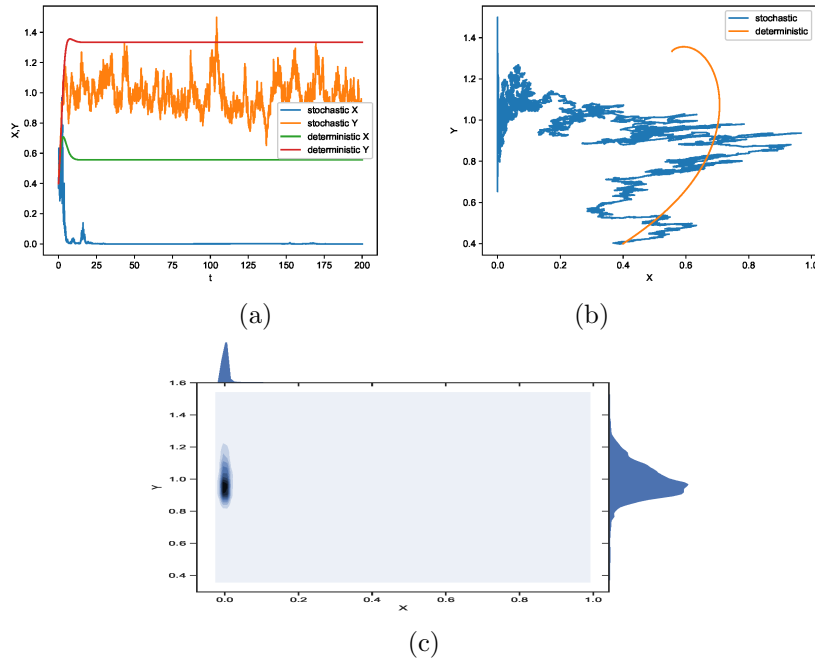


FIGURE 17. Numerical solutions to (3.6) with initial value $(X_0, Y_0) = (0.4, 0.4)$ and parameters $\rho_1 = 1, \mu_1 = \mu_2 = \rho_2 = 0.1$: (a) trajectories of solutions; (b) phase portrait; (c) top, right and inside of the box are the marginal and joint density distribution of solution (X, Y) , respectively.

$\check{\Omega}_x = \{\ln X_{1,x}(T) - \ln x \geq \frac{1}{4}a_1T\}$. Moreover, there are $T = T(\varsigma)$ and $\tilde{\delta}_2(\varsigma) > 0$ such that

$$\limsup_{N \rightarrow \infty} \frac{1}{N} \sum_{k=0}^{N-1} \mathbb{P} \left\{ X_{1,x}(kT) \leq \tilde{\delta}_2 \right\} \leq \varsigma \quad \text{for all } x \in \mathbb{R}_+^{2,\circ}. \tag{5.2}$$

Proof. By the exponential martingale inequality, we have $\mathbb{P}(\Omega_{10}^x) \geq 1 - \varsigma$, where

$$\Omega_{10}^x = \left\{ \int_0^t \mu_2 \psi_{2,x}(s) dW_2(s) \leq \ln \frac{1}{\varsigma} + \frac{1}{2} \int_0^t \mu_2^2 \psi_{2,x}^2(s) ds \right\}.$$

It follows from Itô's formula that for $\omega \in \Omega_{10}^x$ and $t > 0$, $\ln \psi_{2,x}(t) \leq \ln x_2 + \ln \frac{1}{\varsigma} + a_2 t$, and hence

$$\limsup_{t \rightarrow \infty} \frac{1}{t} \ln \psi_{2,x}(t) \leq a_2 < 0,$$

which implies that $\lim_{t \rightarrow \infty} \psi_{2,x}(t) = 0$ almost surely. There exists $T_3 > 0$ such that $\mathbb{P}(\Omega_{11}^x) \geq 1 - \varsigma$, where

$$\Omega_{11}^x = \left\{ \frac{1}{T_3} \int_0^{T_3} \left(a_1 - c_1(\psi_{2,x}(t) + \hat{\nu}) - \frac{\rho_1^2}{2}(\psi_{2,x}(t) + \hat{\nu})^2 \right) dt \geq \frac{3}{4}a_1 \right\}.$$

It follows from Lemma 4.3 that we can choose $\check{\sigma} = \check{\sigma}(\varsigma, R) > 0$ such that $b_1 \check{\sigma} + \frac{1}{2} \mu_1^2 \check{\sigma}^2 \leq a_1/4$ and $\mathbb{P}(\Omega_{12}^x) \geq 1 - \varsigma$, where $\Omega_{12}^x = \{|\psi_{2,x}(t) - X_{2,x}(t)| < \hat{\nu} \text{ for all } t \in$

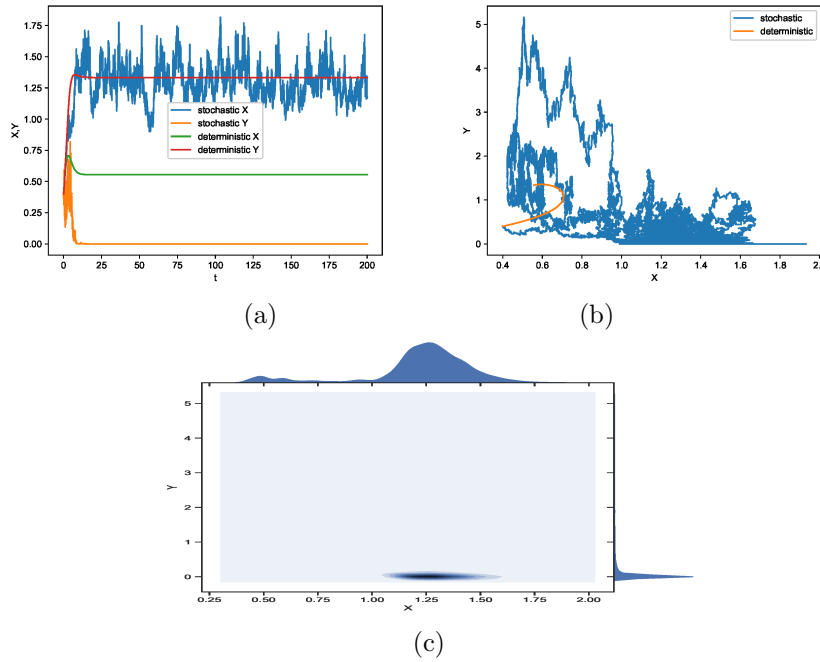


FIGURE 18. Numerical solutions to (3.6) with initial value $(X_0, Y_0) = (0.4, 0.4)$ and parameters $\rho_2 = 1.1, \mu_1 = \mu_2 = \rho_1 = 0.1$: (a) trajectories of solutions; (b) phase portrait; (c) top, right and inside of the box are the marginal and joint density distribution of solution (X, Y) , respectively.

$[0, T_3 \wedge \tau_{1,x}^{\check{\sigma}}]$. Lemma 4.2 implies that there exists $\delta = \delta(\varsigma, R)$ such that $\mathbb{P}(\Omega_{13}^x) \geq 1 - \varsigma$ for all $x \in D_1^{R,\delta}$, where $\Omega_{13}^x = \{\tau_{1,x}^{\check{\sigma}} \geq T_3\}$. Let $T_4 > 16\widehat{M}^2 R / (\varsigma^2 a_1^2)$, then it follows that $\mathbb{P}(\Omega_{14}^x) \geq 1 - \varsigma$, where

$$\Omega_{14}^x = \left\{ \left| \int_0^{T_5} \mu_1 X_{1,x}(t) dW_1(t) + \rho_1 X_{2,x}(t) dW_3(t) \right| \leq \frac{a_1}{4} T_4 \right\}.$$

Let $T = T_3 \wedge T_4$, then applying Itô's formula to the first equation of (1.4) yields that $\ln X_{1,x}(T) - \ln x_1 > \frac{1}{4} a_1 T$ for $x \in D_1^{R,\delta}$ and $\omega \in \check{\Omega}^x = \cap_{i=10}^{14} \Omega_i^x$. Consequently, $\mathbb{P}(\check{\Omega}^x) > 1 - \varsigma$. Similarly to [23, Proposition 3.2], we conclude that there are $T = T(\varsigma) > 0$ and $\tilde{\delta}_2 = \tilde{\delta}_2(\varsigma) > 0$ such that (5.2) holds, which implies that $X_{1,x}$ is away from zero for all $x \in \mathbb{R}_+^{2,0}$. The proof is complete. \square

Proof of Theorem 2.2(i). It is easy to see that there exists $R > 1$ such that

$$\limsup_{t \rightarrow \infty} \mathbb{P}\{X_x(t) \in C\} \geq 1 - \varsigma, \tag{5.3}$$

where $C \triangleq \{R^{-1} \leq x_1 \vee x_2 \leq R\}$. By Lemma 5.1, there exists $\tilde{\delta} > 0$ such that

$$\mathbb{P}\left\{ \limsup_{t \rightarrow \infty} \frac{1}{t} \ln X_{2,x}(t) \leq -\lambda \text{ and } |\Phi_{1,x}(t)| < \gamma' \right\} \geq 1 - 3\varsigma \tag{5.4}$$

for all $x \in D_2^{R, \tilde{\delta}}$. By Lemma 5.2, there exist $T_5 > 1$ and $\tilde{\delta}_2 > 0$ such that

$$\limsup_{N \rightarrow \infty} \frac{1}{N} \sum_{i=0}^{N-1} \mathbb{P}\{X_{1,x}(iT_5) < \tilde{\delta}_2\} \leq \varsigma. \tag{5.5}$$

Using a similar arguments as in the proof of Theorem 2.1(ii), we can find i_0 such that $\mathbb{P}\{X_x(i_0T_5) \in D_2^{R, \tilde{\delta}}\} \geq 1 - 3\varsigma$, which together with (5.4) and Markov property implies that

$$\mathbb{P}\left\{ \limsup_{t \rightarrow \infty} \frac{1}{t} \ln X_{2,x}(t) \leq -\lambda \right\} \geq (1 - 3\varsigma)^2 \geq 1 - 6\varsigma.$$

Namely, $X_{2,x}(t)$ goes to extinction. The convergence of $X_{1,x}(t)$ to π_1^* can be obtained by a similar method to Theorem 2.1(ii) as well. The proof is complete. \square

Lemma 5.3. *If $a_1 > 0 > a_2$ and $\lambda_1 > 0$ then then for any $\varsigma > 0$, $R > 1$, there are $T = T(\varsigma, R) > 0$ and $\delta_0 = \delta_0(\varsigma, R)$ such that $\mathbb{P}(\widehat{\Omega}^x) > 1 - 4\varsigma$ for all $x = (x_1, x_2) \in D_2^{R, \delta_0}$, where $\widehat{\Omega}^x = \{\ln X_{2,x}(T) - \ln x_2 \geq \frac{1}{7}\lambda_1 T\}$. Moreover, there are $T = T(\varsigma)$ and $\delta_2 = \delta_2(\varsigma) > 0$ such that*

$$\limsup_{N \rightarrow \infty} \frac{1}{N} \sum_{k=0}^{N-1} \mathbb{P}\{X_{2,x}(kT) \leq \delta_2\} \leq \varsigma \text{ for all } x \in \mathbb{R}_+^{2,\circ}. \tag{5.6}$$

Proof. In view of the definition of λ_1 , we have

$$a_2 + \int_0^\infty [c_2(u - \nu) - \frac{\rho_2^2}{2}(u + \nu)^2] f_1^*(u) du \geq \frac{2\lambda_1}{3}$$

for sufficiently small ν . It follows from the ergodicity of $\psi(t)$ that there is $T = T(\varsigma, R) > 1746\widehat{M}^2 R / (\varsigma^2 \lambda_1^2)$ such that

$$\mathbb{P}\left\{ a_2 + \frac{1}{T} \int_0^T [c_2(\psi_{1,R^{-1}}(s) - \nu) - \frac{\rho_2^2}{2}(\psi_{1,R}(s) + \nu)^2] ds \geq \frac{\lambda_1}{2} \right\} \geq 1 - \varsigma.$$

By the uniqueness of solution, $\psi_{1,R^{-1}}(t) \leq \psi_{1,x}(t) \leq \psi_{1,R}(t)$ a.s. for all $x \in [R^{-1}, R]$. Thus, we have $\mathbb{P}(\Omega_{15}^x) \geq 1 - \varsigma$, where

$$\Omega_{15}^x = \left\{ a_2 + \frac{1}{T} \int_0^T [c_2(\psi_{1,x}(s) - \nu) - \frac{\rho_2^2}{2}(\psi_{1,x}(s) + \nu)^2] ds \geq \frac{\lambda_1}{2} \right\}.$$

In view of Lemma 4.3, there is $\sigma > 0$ such that $b_2\sigma + \frac{1}{2}\mu_2^2\sigma^2 \leq \frac{\lambda_1}{3}$ and $\mathbb{P}(\Omega_{16}^x) \geq 1 - \varsigma$, where

$$\Omega_{16}^x = \{ |\psi_{1,x}(t) - X_{1,x}(t)| < \nu \text{ for all } t \in [0, T \wedge \tau_{2,x}^\sigma] \}.$$

It follows from Lemma 4.2 that there exists $\delta_0 = \delta_0(\varsigma, R)$ such that $\mathbb{P}(\Omega_{17}^x) \geq 1 - \varsigma$ for all $x \in D_2^{R, \delta_0}$, where $\Omega_{17}^x = \{\tau_{2,x}^\sigma \geq T\}$. Using a similar argument as the proof of Lemma 4.4, we have $\mathbb{P}(\Omega_{18}^x) \geq 1 - \varsigma$, where

$$\Omega_{18}^x = \left\{ \left| \int_0^T \mu_2 X_{2,x}(s) dW_2(s) + \rho_2 X_{1,x}(s) dW_3(s) \right| \leq \frac{\lambda_1}{42} T \right\}.$$

Applying Itô's formula to the second equation of (1.4) yields that for $x \in D_2^{R, \delta_0}$ and $\omega \in \widehat{\Omega}^x = \cap_{i=15}^{18} \Omega_i^x$,

$$\ln X_{2,x}(T) - \ln x_2 \geq \int_0^T [a_2 + c_2(\psi_{1,x}(s) - \nu) - \frac{\rho_2^2}{2}(\psi_{1,x}(s) + \nu)^2] dt - \frac{5\lambda_1}{14}$$

$$\geq \frac{\lambda_1}{7}T.$$

Consequently, we obtain $\mathbb{P}(\widehat{\Omega}^x) > 1 - 4\varsigma$. Similarly to [23, Proposition 3.2], we conclude that there are $T = T(\varsigma)$ and $\delta_2 = \delta_2(\varsigma) > 0$ such that (5.6) holds, which implies that $X_{2,x}$ is away from zero for all $x \in \mathbb{R}_+^{2,\circ}$. \square

Proof of Theorem 2.2(ii). Lemma 5.3 implies that $X_{2,x}$ is away from zero for all $x \in \mathbb{R}_+^{2,\circ}$. If $\mathbb{P}\{\omega : \lim_{t \rightarrow \infty} X_{1,x}(t) = 0\} > 0$, then it follows from (4.4) that

$$\mathbb{P}\left(\limsup_{t \rightarrow \infty} \frac{1}{t} \ln X_{2,x}(t) < 0\right) > 0,$$

which contradicts Lemma 5.3, and hence that almost surely $\limsup_{t \rightarrow \infty} X_{1,x}(t) > 0$. In view of Lemma 4.1, there exists a constant $C > 0$ such that

$$\frac{1}{t} \int_0^t \mathbb{E}(X_{1,x}^p(s) + X_{2,x}^p(s)) ds \leq C.$$

According to in [4, Theorem 4.14], there exists a stationary distribution for $X_x(t)$. This completes the proof. \square

6. PROOF OF THEOREM 2.4

This section is devoted to the case where both the predator population and the prey population have positive intrinsic growth rates, that is, $a_1 > 0$ and $a_2 > 0$.

Lemma 6.1. *Assume that $a_2 > 0$ and $\lambda_2 < 0$, then for any $R > 1$, $\varsigma, \gamma > 0$, there exists $\hat{\delta} > 0$ such that for all $x \in D_1^{R,\hat{\delta}}$,*

$$\mathbb{P}\left\{\limsup_{t \rightarrow \infty} \frac{1}{t} \ln X_{1,x}(t) \leq 0 \text{ and } |\Phi_{2,x}(t)| < \gamma\right\} \geq 1 - 3\varsigma.$$

The proof of the above lemma is similar to that of Lemma 5.1 and hence we omit it. By Lemmas 4.3 and 5.3, using a similar method to Theorem 2.2, we can prove Theorem 2.4(i)(ii). Note that if $\lambda_1 > 0$ and $\lambda_2 > 0$, there exist $T_7 > 1$ and $\tilde{\delta}_2 > 0$ such that

$$\limsup_{N \rightarrow \infty} \frac{1}{N} \sum_{i=0}^{N-1} \mathbb{P}\{|X_{1,x}(iT_7)| \wedge |X_{2,x}(iT_7)| < \tilde{\delta}_2\} \leq 2\varsigma. \quad (6.1)$$

The proof of Theorem 2.4(iii) is similar to the proof of Theorem 2.2(ii).

Acknowledgements. This work was partially supported by the National Natural Science Foundation of China (Grant Nos. 12071446 & 12101578), Natural Science Foundation of Hubei (Grant No. 2021CFB167), China Postdoctoral Science Foundation (Grant No. 2020M682507), the Post-doctoral Innovative Research Positions in Hubei Province, China (Grant No. 260789), and the Fundamental Research Funds for the Central Universities, China University of Geosciences (Wuhan) (Grant No. CUGST2).

REFERENCES

- [1] L. J. S. Allen; *An Introduction to Stochastic Processes with Applications to Biology*, Person Prentice Hall, 2003.
- [2] L. Arnold, W. Horsthemke, J. W. Stucki; *The influence of external real and white noise on the Lotka-Volterra model*, Biometrical Journal, **21**(5) (1979), 451–471.
- [3] Y. T. Cai, C. C. Wang, D. Fan; *Stability and bifurcation in a delayed predator-prey model with Holling-type IV response function and age structure*, Electronic Journal of Differential Equations, **2021** (2021), no. 42, 1–16.
- [4] M. Chen; *From Markov chains to non-equilibrium particle systems*, World Scientific, 2004.
- [5] N. H. Dang, N. H. Du, T. V. Ton; *Asymptotic behavior of predator-prey systems perturbed by white noise*, Acta Applicandae Mathematicae, **115** (2011), 351–370.
- [6] J. Gao, S. Guo; *Global dynamics and spatio-temporal patterns in a two-species chemotaxis system with two chemicals*, Zeitschrift für angewandte Mathematik und Physik **72** (2021), 25.
- [7] D. J. Higham; *An algorithmic introduction to numerical simulation of stochastic differential equations*, SIAM Review, **43** (2001), 525–546.
- [8] C. Ji, D. Jiang; *Dynamics of a stochastic density dependent predator-prey system with Beddington-DeAngelis functional response*, Journal of Mathematical Analysis and Applications, **381** (2011), 441–453.
- [9] D. Jiang, C. Ji, X. Li, D. O’Regan; *Analysis of autonomous Lotka-Volterra competition systems with random perturbation*, Journal of Mathematical Analysis and Applications, **390**(2) (2012), 582–595.
- [10] S. Li, S. Guo; *Permanence of a stochastic prey-predator model with a general functional response*, Mathematics and Computers in Simulation, **187** (2021), 308–336.
- [11] S. B. Li, Y. Xiao, Y. Dong; *Diffusive predator-prey models with fear effect in spatially heterogeneous environment*, Electronic Journal of Differential Equations, **2021** (2021), no. 70, 1–31.
- [12] X. Li, D. Jiang, X. Mao; *Population dynamical behavior of Lotka-Volterra system under regime switching*, Journal of Computational and Applied Mathematics, **232**(2) (2009), 427–448.
- [13] C. Liu, S. Guo; *Steady states of Lotka-Volterra competition models with nonlinear cross-diffusion*, Journal of Differential Equations, **292**(2021), 247–286.
- [14] Q. Liu, D. Q. Jiang, T. Hayat, B. Ahmad; *Stationary distribution and extinction of a stochastic predator-prey model with additional food and nonlinear perturbation*, Applied Mathematics and Computation, **320** (2018), 226–239.
- [15] C. Lu, X. H. Ding; *Periodic solutions and stationary distribution for a stochastic predator-prey system with impulsive perturbations*, Applied Mathematics and Computation, **350** (2019), 313–322.
- [16] Q. Luo, X. Mao; *Stochastic population dynamics under regime switching*, Journal of Mathematical Analysis and Applications, **334**(1) (2007), 69–84.
- [17] J. Lv, K. Wang; *Asymptotic properties of a stochastic predator-prey system with Holling II functional response*, Communications in Nonlinear Science and Numerical Simulation, **16** (2011), 4037–4048.
- [18] L. Ma, S. Guo; *Positive solutions in the competitive Lotka-Volterra reaction-diffusion model with advection terms*, Proceedings of the American Mathematical Society, **149**(7) (2021), 3013–3019.
- [19] L. Ma, S. Guo; *Bifurcation and stability of a two-species reaction-diffusion-advection competition model*, Nonlinear Analysis: Real World Applications **59** (2021), 103241.
- [20] X. Mao, G. Marion, E. Renshaw; *Environmental Brownian noise suppresses explosions in population dynamics*, Stochastic Processes and their Applications, **97**(1) (2002), 95–110.
- [21] X. Mao, S. Sabais, E. Renshaw; *Asymptotic behavior of stochastic Lotka-Volterra model*, Journal of Mathematical Analysis and Applications, **287** (2003), 141–156.
- [22] J. Murray; *Mathematical Biology I: An Introduction*, (3rd Edition), Springer-Verlag, 2002.
- [23] D. H. Nguyen, G. Yin; *Coexistence and exclusion of stochastic competitive Lotka-Volterra models*, Journal of Differential Equations, **262** (2017), 1192–1225.
- [24] K. Nosrati, M. Shafiee; *Dynamic analysis of fractional-order singular Holling type-II predator-prey system*, Applied Mathematics and Computation, **313** (2017), 159–179.

- [25] M. Q. Ouyang, X. Y. Li; *Permanence and asymptotical behavior of stochastic prey-predator system with Markovian switching*, Applied Mathematics and Computation, **266** (2015), 539–559.
- [26] H. Qiu, S. Guo, S. Li; *Stability and bifurcation in a predator-prey system with prey-taxis*, International Journal of Bifurcation and Chaos, **30** (2) (2020), 2050022
- [27] R. Rudnicki; *Long-time behaviour of a stochastic prey-predator model*, Stochastic Processes and their Applications, **108** (2003), 93–107.
- [28] R. Rudnicki, K. Pichór; *Influence of stochastic perturbation on prey-predator systems*, Mathematical Biosciences, **206** (2007), 108–119.
- [29] R. Rudnicki, K. Pichór, M. Tyran-Kaminska; *Markov semigroups and their applications*. In: Garbaczewski, P., Olkiewicz, R. (eds.) Dynamics of Dissipation. Lecture Notes in Physics, Springer, Berlin, **597** (2002), 215–238.
- [30] F. Vadillo; *Comparing stochastic Lotka-Volterra predator-prey models*, Applied Mathematics and Computation, **360** (2019), 181–189.
- [31] A. Yagi, T. V. Ton; *Dynamic of a stochastic predator-prey population*, Applied Mathematics and Computation, **218** (2011), 3100–3109.
- [32] Y. Zhu, M. Liu; *Permanence and extinction in a stochastic service-resource mutualism model*, Applied Mathematics Letters, **69** (2017), 1–7.

SHANGZHI LI

CENTER FOR MATHEMATICAL SCIENCES, CHINA UNIVERSITY OF GEOSCIENCES, WUHAN, HUBEI
430074, CHINA

Email address: lishangzhi@cug.edu.cn

SHANGJIANG GUO (CORRESPONDING AUTHOR)

SCHOOL OF MATHEMATICS AND PHYSICS, CHINA UNIVERSITY OF GEOSCIENCES, WUHAN, HUBEI
430074, CHINA

Email address: guosj@cug.edu.cn